

ISSN 3088-3083 (Print)
ISSN 3088-3059 (Online)



จักษุเวชสาร

THE THAI JOURNAL OF OPHTHALMOLOGY

Vol. 39 No. 2 July - December 2025

Original Articles

Choroidal Vascularity Index Changes after Treatment of Persistent Central Serous Chorioretinopathy with either Spironolactone or Half-Dose Photodynamic Therapy

Wongsiri Taweebanjongsin, MD, Sitthipol Piriyakootorn, MD, Karntida Chanwimol, MD, Julaporn Pooliam, MD, Rupesh Agrawal, MD, Srinivas R Sadda, MD

Effects of Dexamethasone Implant on Contralateral Central Foveal and Subfoveal Choroidal Thickness in Unilateral Uveitic Macular Edema

Mukaddes Damla Ciftci, MD, Mine Esen Baris, MD, Suzan Guven, MD

Case Reports

Acute Unilateral Isolated Ptosis as a Complication of Frontal Sinusitis: A Case Report

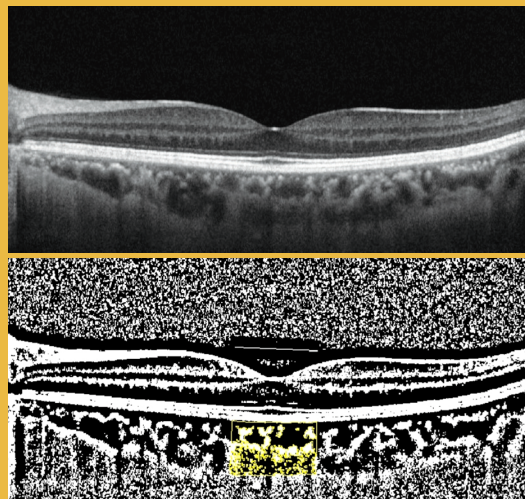
Busayanut Puangsricharoen, MD

Adult Orbital Xanthogranuloma: A Case Report

Paphitchaya Temphattharachok, MD, Monkol Uiprasertkul, MD, Sunisa Sintuwong, MD, MPPM, MSc

Specific Ocular Findings Leading to the Diagnosis of Early-Onset Neurofibromatosis Type 2

Pittaya Phamonvaechavan, MD, Subongkoch Subhadhirasakul MD, Rawi Jongpipatchai, MD, Supathida Jiamsawad, MD





จักษุเวชสาร

The Thai Journal of Ophthalmology

คณะกรรมการบริหารราชวิทยาลัยจักษุแพทย์แห่งประเทศไทย

วาระปี 2568 – 2569

ประธาน	นพ.ปานเนตร ปางพุฒิพงศ์
ที่ปรึกษาคณะกรรมการวิจัย	ศ.เกียรติคุณ นพ.ยศอนันต์ ยศไพบุลย์
ที่ปรึกษาด้านฝึกอบรมและสอบฯ และ คณะกรรมการด้านสาธารณสุข รองประธาน และประธานคณะกรรมการจริยธรรม	ศ.เกียรติคุณ พญ.วณิษา ชื่นก่องแก้ว รศ.นพ.อนุชิต ปุญญทลิ่งค์
เลขาธิการ	พ.อ.นพ.ยุทธพงษ์ อิมสุวรรณ
เหรียญกิตติมศักดิ์	ศ.นพ.นิพนธ์ จิรภาไพศาล
ประธานคณะกรรมการฝึกอบรมและสอบฯ	พ.อ.หญิง ผศ.พญ.รวิวรรณ ชุนถนอม
ประธานวิชาการและกิจกรรมสังคม	รศ.นพ.ศักดิ์ชัย วงศกิตติรักษ์
ประธานคณะกรรมการวิจัย	ศ.พญ.เกวลิณ เลขานนท์
ประธานคณะกรรมการเทคโนโลยีสารสนเทศ	นพ.ธนาพงษ์ สมกิจรุ่งโรจน์
ประธานฝ่ายวิชาชีพ	รศ.พญ.มัญชิมา มะกรวัฒนะ
ประธานคณะกรรมการนวัตกรรมและเทคโนโลยี กรรมการกลาง	ศ.พญ.สุภาภรณ์ เตังไตรสรณ์ นพ.พิพัฒน์ คงทรัพย์ รศ.พญ.กนกรัตน์ พรพาณิชย์ ศ.พญ.วสี ตูลวรรณะ รศ.นพ.ดิเรก ผาติกุลศิลา ศ.นพ.แมนสิงห์ รัตนสุคนธ์ พ.อ.หญิง ผศ.พญ.ฐิติพร รัตนพจนารถ พญ.รัตติยา พรชัยสุรีย์ ผศ.พญ.ธารสุข เกษมทรัพย์ นพ.เอกชัย อารยางกูร ผศ.นพ.ธนภัทร รัตนภากร รศ.นพ.ณวพล กาญจนารัตน์ น.อ.นพ.วรัศม์ภรณ์ พลอยประสิทธิ์



จักษุเวชสาร

The Thai Journal of **Ophthalmology**

The Royal College Executive Committee

2025 – 2026

President

Pannet Pangputhipong, MD

Advisory of Research Subcommittee

Yosanan Yospaiboon, MD

Advisory of Training and Public Health Subcommittee

Wanicha Chuenkongkaew, MD

Vice-President and Chair of Ethical Subcommittee

Anuchit Poonyathalang, MD

Secretary

Yutthaphong Imsuwan, MD

Treasurer

Niphon Chirapapaisan, MD

Chair of Training and Examination Subcommittee

Raveewan Choontanom, MD

Scientific Committee

Sakchai Vongkittirux, MD

Chair of Research Subcommittee

Kaevalin Lekhanont, MD

Chair of Information Technology Subcommittee

Thanapong Somkijrungrroj, MD

Chair of International Affair

Manchima Makornwattana, MD

Chair of Innovation and Technology Subcommittee

Supaporn Tengtrisorn, MD

Committee Member

Pipat Kongsap, MD

Kanokrat Pornpanich, MD

Wasee Tulvatana, MD

Direk Patikulsila, MD

Mansing Ratanasukon, MD

Thitiporn Ratanapojnard, MD

Rattiya Pornchaisuree, MD

Tharnsook Kasemsup, MD

Ekkachai Arayangkul, MD

Thanapat Rattanapakorn, MD

Navapol Kanchanaranya, MD

Warathporn Ployprasith, MD

คณะอนุกรรมการวิชาการและกิจกรรมสังคม (Scientific and Social Activities Subcommittee)

รศ.นพ.ศักดิ์ชัย วงศกิตติรักษ์
นพ.ธนาพงษ์ สมกิจรุ่งโรจน์
นพ.วรภัทร วงษ์สวัสดิ์
นพ.ดวงมนตรี โรจน์ดำรงรัตนา
นพ.สุวิช รัตนศิรินทรูธ
ศ.นพ.นิพนธ์ จิรภาไพศาล
รศ.พญ.วิศนี ตันติเสวี
รศ.พญ.ญาณิน สุวรรณ
ศ.ดร.พญ.เกษรา พัฒนพิฑูรย์
พญ.ภาวสุทธิ์ สุภาสัย
รศ.พญ.วันทนีย์ สิทธิวารกุล
พญ.ภรณ์ลดา ศัลกวิเศษ
พันเอก พญ.วิวรรณ คันสนยุท
รศ.นพ.ณวพล กาญจนารัตน์
พญ.อรวิณัฐ นิมิตวงศ์สกุล
น.อ.ต.นพ.เกษม ยศไพบูลย์
ผศ.นพ.ดำรงค์ วิวัฒน์วงศ์วนา
นพ.ธีรศักดิ์ พิพัฒน์นเรศวร
ผศ.นพ.นิพัฒน์ เอื้ออารี
รศ.(พิเศษ) พญ.อุษณีย์ เจริญประยูร
ผศ.พญ.พิมพ์ขวัญ จารุอำพรพรรณ
รศ.พญ.สุพินดา ลีอมรสิริ
ผศ.พญ.พรรณทิพา ว่องไว
นพ.พิพัฒน์ คงทรัพย์
พญ.กุลวรรณ โรจน์เนืองนิตย์
รศ.ดร.นพ.นพศักดิ์ ผาสุกกิจวัฒนา
รศ.นพ.ยอดพงศ์ จันทรส
อ.นพ.ธนิต วงษ์วิบูลย์สิน

Sakchai Vongkittirux, MD
Thanapong Somkijrungrroj, MD
Warrapat Wongsawad, MD
Duangmontree Rojdamrongratana, MD
Suwich Ratanasirintrawoot, MD
Niphon Chirapapaisan, MD
Visanee Tantisevi, MD
Yanin Suwan, MD
Kessara Pathanapitoon, MD
Pawasoot Supasai, MD
Wantanee Sittivarakul, MD
Pornlada Sunlakaviset, MD
Wiwan Sansanayudh, MD
Navapol Kanchanaranya, MD
Ornvenus Nimitwongsakul, MD
Kasem Yospaiboon, MD
Damrong Wiwatwongwana, MD
Dhirasak Pipatnoraseth, MD
Nipat Aui-aree, MD
Usanee Reinprayoon, MD
Pimkwan Jaru-Ampornpan, MD
Supinda Leeamornsiri, MD
Pantipa Wongwai, MD
Pipat Kongsap, MD
Kulawan Rojananuangnit, MD
Nopasak Phasukkijwatana, MD
Yodpong Chantarasorn, MD
Tanit Wongwibulsin, MD

คณะกรรมการฝึกอบรมและสอบฯ สาขาจักษุวิทยา (Training and Examination Subcommittee)

ศ.เกียรติคุณ พญ.วณิชา ชื่นกองแก้ว <i>ที่ปรึกษา</i>	Wanicha Chuenkongkaew, MD <i>Advisory</i>
ผศ.พอ.พญ.รวิวรรณ ชุนถนอม	Raveewan Choontanom, MD
รศ.นพ.ศักดิ์ชัย วงศกิตติรักษ์	Sakchai Vongkittirux, MD
พญ.ดวงดาว ทัดณรงค์	Duangdao Thatsnarong, MD
พ.อ. พญ.คณิสสภณา กล้าณรงค์ราญ	Kanaspana Klanarongran, MD
รศ.นพ.พิทยา งามรวชวรรณ	Pittaya Phamonvaechavan, MD
รศ.พญ.อนิตา มนัสสากร	Anita Manassakorn, MD
ศ.พญ.ภารดี คุณาวิศรุต	Paradee Kunavisarut, MD
รศ.พญ.สุธาสินี สีนะวัฒน์	Suthasinee Sinawat, MD
ผศ.พิเศษ พญ.สมพร จันทรา	Somporn Chantra, MD
น.ท.นพ.วรัศม์ภรณ์ พลอยประสิทธิ์	Warassabhorn Ployprasith, MD
ผศ.นพ.วสุ ศุภภรณ์สาร	Wasu Supakontanasan, MD
พญ.กรวิภา เหมะรัต	Kornwipa Hemarat, MD
พญ.วันทนี้อย่าง บุญชีมิ	Wantanee Dangboon Thuthumi, MD
น.ต.อ.นพ.เกษม ยศไพบูลย์	Kasem Yospaiboon, MD
ผศ.พิเศษ พญ.วรรณกรณ์ พฤกษากร	Vannakorn Pruksakorn, MD

คณะกรรมการวิจัย (Research Subcommittee)

ศ.เกียรติคุณ นพ.ยศอนันต์ ยศไพบูลย์ <i>ที่ปรึกษา</i>	Yosanan Yospaiboon, MD <i>Advisory</i>
รศ.นพ.ภฤศ หาญอุตสาหะ <i>ที่ปรึกษา</i>	Prut Hanutsaha, MD <i>Advisory</i>
ศ.พญ.เกวลิณ เลขานนท์	Kaevalin Lekhanont, MD
รศ.พญ.เจนจิต ชูอุดมยากร	Janejit Choovuthayakorn, MD
รศ.นพ.ปิติพล ชูพงศ์	Pitipol Choopong, MD
รศ.นพ.โกศล คำพิทักษ์	Kosol Kampitak, MD
นพ.พิพัฒน์ คงทรัพย์	Pipat Kongsap, MD
รศ.(พิเศษ) พญ.อุษณีย์ เหมียญประยูร	Usanee Reinprayoon, MD
รศ.ดร.พญ.ภัศรา จงขจรพงษ์	Passara Jongkhajornpong, MD
ผศ.พญ.สิรินยา สุวรรณราช	Sirinya Suwannaraj, MD
รศ.นพ.ยอดพงศ์ จันทรร	Yodpong Chantarasorn, MD
ผศ.พญ.พรรณรพี ฟูณานารถ	Panrapee Funarunart, MD
รศ.พญ.อรพรรณ อาญาสิทธิ์	Orapan Aryasit, MD
พญ.วรุณกานต์ รุ่งภูวภัทร	Vatookarn Roongpuwapatara, MD
น.ต.อ.นพ.เกษม ยศไพบูลย์	Kasem Yospaiboon, MD
พญ.ปาริณา ชัยทรวงศ์	Pareena Chaitanuwong, MD

คณะกรรมการนวัตกรรมและเทคโนโลยี (Innovation and Technology Subcommittee)

ศ.พญ.สุภาภรณ์ เต็งไตรสรณ์

รศ.พญ.วิภาวี บูรณพงศ์

รศ.นพ.ธรรศ สงวนศักดิ์

รศ.พญ.สุภรัตน์ จรรย์โกศล

รศ.พญ.อรพรรณ อาญาสิทธิ์

นพ.ลั่นหล้า อุดมเวช

พญ.ปัญญนุช พิสิฐพยัต

นพ.เกษม เสรีศิริขจร

รศ.นพ.ณวพล กาญจนารัณย์

Supaporn Tengtrisorn, MD

Wipawee Booranapong, MD

Thuss Sanguansak, MD

Supharat Jariyakosol, MD

Orapan Aryasit, MD

Lunla Udomwech, MD

Punyanuch Pisitpayat, MD

Kasem Seresirikachorn, MD

Navapol Kanchanaranya, MD



จักษุเวชสาร

The Thai Journal of Ophthalmology

จักษุเวชสาร เป็นวารสารของราชวิทยาลัยจักษุแพทย์แห่งประเทศไทย และสมาคมจักษุแพทย์แห่งประเทศไทย

คณะกรรมการจักษุเวชสาร

บรรณาธิการ

ศ.พญ.เกวณีน เลขานนท์

คณะแพทยศาสตร์โรงพยาบาลรามาธิบดี

ผู้ช่วยบรรณาธิการ

พญ.ปริญญช พิสิฐพยัคฆ์

คณะแพทยศาสตร์วชิรพยาบาล มหาวิทยาลัยนวมินทราธิราช

กองบรรณาธิการ

ศ.เกียรติคุณ พญ.วณิษา ชื่นกองแก้ว

คณะแพทยศาสตร์ศิริราชพยาบาล

ศ.พญ.ภิญญา ตันธวัณนิตย์

คณะแพทยศาสตร์ศิริราชพยาบาล

รศ.นพ.สมเกียรติ อัครวารีกรรม

คณะแพทยศาสตร์ มหาวิทยาลัยขอนแก่น

รศ.นพ.วินัย ชัยตระกูล

คณะแพทยศาสตร์ มหาวิทยาลัยเชียงใหม่

ศ.นพ.แมนสิงห์ รัตนสุคนธ์

คณะแพทยศาสตร์ มหาวิทยาลัยสงขลานครินทร์

ผศ.พอ.หญิง พญ.รวีวรรณ ชุนถนอม

โรงพยาบาลพระมงกุฎเกล้า

ศ.(พิเศษ) นพ.บุญสูง วนิชเวชารุ่งเรือง

โรงพยาบาลราชวิถี

นพ.ปานเนตร ปางพุฒิพงศ์

โรงพยาบาลเมตตาประชารักษ์ (วัดไร่ขิง)

รศ.(พิเศษ) พญ.โสฬส วุฒิพันธุ์

สถาบันจักษุวิทยา โรงพยาบาลสงฆ์

Professor Harold Furr

USA

ที่ปรึกษากิตติมศักดิ์

ศ.นพ.พรชัย สิมะโรจน์

คณะแพทยศาสตร์โรงพยาบาลรามาธิบดี

ศ.เกียรติคุณ นพ.ยศอนันต์ ยศไพบูลย์

คณะแพทยศาสตร์ มหาวิทยาลัยขอนแก่น

รศ.นพ.ภฤศ หาญอุตสาหะ

คณะแพทยศาสตร์โรงพยาบาลรามาธิบดี

เจ้าหน้าที่ประสานงาน

คุณสุวิช ศรีประดิษฐ์

จักษุเวชสาร เป็นวารสารที่มีการทบทวนโดยผู้ใ้เสมอ (Peer-review) เผยแพร่แบบฉบับตีพิมพ์ (ISSN 3088-3083) และแบบออนไลน์ (ISSN 3088-3059) จัดทำปีละสองฉบับ มีวัตถุประสงค์เพื่อให้ความรู้ในสาขาจักษุวิทยาที่ทันสมัย สนับสนุนการเรียนรู้ต่อเนื่องทางการแพทย์ เอื้อให้เกิดความร่วมมือ และแลกเปลี่ยนทัศนะในหมู่สมาชิกราชวิทยาลัย และผู้อ่าน

สำนักงาน

ราชวิทยาลัยจักษุแพทย์แห่งประเทศไทย ชั้น 10 อาคารเฉลิมพระบารมี 50 ปี

เลขที่ 2 ซอยศูนย์วิจัย ถนนเพชรบุรีตัดใหม่ กรุงเทพมหานคร 10310

โทรศัพท์ 027180715-6 อีเมล: admin@rcopt.org

ออกแบบและพิมพ์ที่

สำนักพิมพ์กรุงเทพเวชสาร 3/3 สุขุมวิท 49 แขวงคลองตันเหนือ เขตวัฒนา กรุงเทพฯ 10110

โทร. 02-2587954 โทรสาร 02-258-7954 E-mail: bkkmed@gmail.com



จักษุเวชสาร

The Thai Journal of Ophthalmology

The Journal of the Royal College of Ophthalmologists and Ophthalmological Society of Thailand

Editor

Kaevalin Lekhanon

Department of Ophthalmology,
Faculty of Medicine Ramathibodi Hospital

Assistant Editor

Punyanuch Pisipayat

Faculty of Medicine Vajira Hospital, Navamindradhiraj University

Editorial Board

Wanicha Cheunkongkaew

Faculty of Medicine Siriraj Hospital

Pinnita Tanthuvanit

Faculty of Medicine Siriraj Hospital

Somkiat Asawaphurikorn

Srinagarind Hospital, Khon Kaen University

Winai Chaidaroon

Faculty of Medicine, Chiangmai University

Mansing Ratanasukon

Faculty of Medicine, Prince of Songkhla University

Raveewan Choontanom

King Mongkut Hospital

Boonsong Wanitwacharungreung

Rajvithi Hospital

Pannet Pangputipong

Metta Pracharak (Wat Rai King) Hospital

Sorot Wuttiphan

Priest Hospital

Professor Harold Furr

USA

Distinguished Advisors

Pornchai Simaraj

Faculty of Medicine Ramathibodi Hospital

Yosanan Yospaiboon

Srinagarind Hospital, Khon Kaen University

Prut Hanutsaha

Faculty of Medicine Ramathibodi Hospital

Administrative Officer

Suwach Sripradit

The Thai Journal of Ophthalmology (TJO) is a peer-reviewed journal, and is published as printed (ISSN 3088-3083) and online journal (ISSN 3088-3059). The TJO is published biannually, and serves the objectives of providing up to date knowledge in the field of Ophthalmology, supports continuing education, promotes cooperation and sharing of opinion among readers.

Office:

The Royal College of Ophthalmologists of Thailand
10th Floor, Royal Golden Jubilee Building,
2 Soi Soonvijai, Petchburi Road, Bangkok 10310
Phone (+66) (0)27180715, (+66) (0)27180716
E-mail: admin@rcopt.org

Designed and printed at:

Bangkok Medical Publisher, Ltd. Part.
3/3 Sukhumvit 49, Khlong Ton Nua, Vadhana, Bangkok 10110
Tel. 02-2587954 E-mail: bkkmed@gmail.com



จักษุเวชสาร

The Thai Journal of Ophthalmology

บรรณาธิการแถลง

จักษุเวชสารฉบับนี้ มีงานวิจัยที่น่าสนใจเกี่ยวกับโรคของจุดรับภาพ และการเปลี่ยนแปลงของชั้น choroid ที่เกี่ยวข้อง ตั้งแต่เรื่องการเปลี่ยนแปลงของ choroidal vascularity index ภายหลังการรักษาโรค persistent central serous chorioretinopathy ด้วยยา spironolactone หรือ half-dose photodynamic therapy และเรื่องผลของ dexamethasone implant ต่อ central foveal และ subfoveal choroidal thickness ของตาข้างตรงข้าม ในผู้ป่วยโรค uveitic macular edema ที่เป็นในตาข้างเดียว ตามมาด้วยรายงานผู้ป่วยที่พบได้น้อยมากอีก 3 รายงาน ได้แก่ ภาวะหนังตาตกข้างเดียวเฉียบพลัน ที่เป็นภาวะแทรกซ้อนจากโรค frontal sinusitis ผู้ป่วยโรค adult orbital xanthogranuloma และผู้ป่วย early-onset neurofibromatosis type 2 ซึ่งมีอาการแสดงจำเพาะทางตาที่นำไปสู่การวินิจฉัยโรคได้ตั้งแต่วัยเริ่มต้น ซึ่งผลงานวิจัยและรายงานผู้ป่วยเหล่านี้อาจเป็นประโยชน์สำหรับสมาชิก ในการนำไปพิจารณาปรับใช้ในการดูแลรักษาผู้ป่วย หรือนำไปศึกษาต่อยอดต่อไปได้

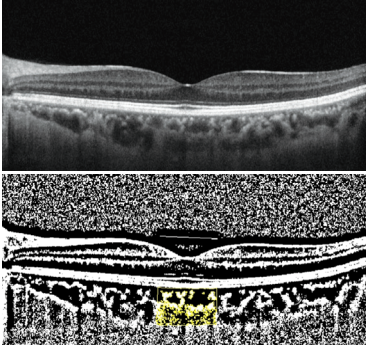
นอกจากนี้เป็นที่น่ายินดีว่า งานวิจัยสองเรื่องที่เป็นนิพนธ์ต้นฉบับ (original article) นั้น มีผู้นิพนธ์จากต่างประเทศร่วมส่งผลงานมารับการพิจารณาตีพิมพ์ในวารสารวิชาการของเรา โดยเรื่องแรกมีผู้นิพนธ์ร่วมจากประเทศสหรัฐอเมริกาและสิงคโปร์ ส่วนเรื่องที่สองเป็นการศึกษาจากประเทศตุรกี จึงถือได้ว่า วารสารวิชาการของเราได้รับความไว้วางใจจากจักษุแพทย์นานาชาติเพิ่มมากขึ้นอย่างต่อเนื่อง นับเป็นการขยายขอบข่ายการเผยแพร่ข้อมูลหรือองค์ความรู้ใหม่ ๆ ผ่านวารสารวิชาการของเราให้กว้างขวางออกไปมากขึ้น เพื่อให้เกิดประโยชน์แก่สมาชิกผู้อ่านสูงสุด

สุดท้ายนี้กองบรรณาธิการยังคงสนับสนุนให้สมาชิกทุกท่าน ส่งผลงานวิจัยในรูปแบบต่าง ๆ รวมถึงรายงานผู้ป่วย หรือการทบทวนวรรณกรรม มาให้กองบรรณาธิการพิจารณาตีพิมพ์ เพื่อช่วยพัฒนามาตรฐานของวารสารของเราให้มีคุณภาพดียิ่ง ๆ ขึ้นไป

กองบรรณาธิการ

ปีที่ 39 ฉบับที่ 2 กรกฎาคม-ธันวาคม 2568

สารบัญ



ภาพปก Enhanced-depth optical coherence tomography central B-scan of the left eye (left panel). Following binarization, the choroid was divided into dark (vascular lumen) and bright (stroma) pixels. A region of interest (highlighted in yellow) with a width of 1,500 μm centered on the foveal center was selected to compute the choroidal vascularity index (CVI).

#Unpaired t-test for continuous data and Chi-square test for categorical data

ix บรรณาธิการแถลง

นิพนธ์ต้นฉบับ

- 61 การศึกษาการเปลี่ยนแปลงของ choroidal vascularity index ในการรักษาโรคจุดภาพชัดแยก
ชั้นจากน้ำรั่วเรื้อรังด้วยสไปโรโนแลคโตนเปรียบเทียบกับการรักษาด้วย photodynamic therapy
วงศ์ศิริ ทวีบรรจงสิน, พ.บ.
สิทธิพล พิริยคุณธร, พ.บ.
กาญจน์ธิดา จันทน์วิมล, พ.บ.
จุฬารัตน์ พูลเอี่ยม, พ.บ.
Rupesh Agrawal, MD
Srinivas R Sadda, MD
- 75 Effects of Dexamethasone Implant on Contralateral Central Foveal and
Subfoveal Choroidal Thickness in Unilateral Uveitic Macular Edema
Mukaddes Damla Ciftci, MD
Mine Esen Baris, MD
Suzan Guven, MD

รายงานผู้ป่วย

- 83 รายงานผู้ป่วย : ภาวะเปลือกตาตกที่เกิดจากโรคไขสันหลังอักเสบ
บุษยณัฐ พวงศรีเจริญ, พ.บ.



จักษุเวชสาร

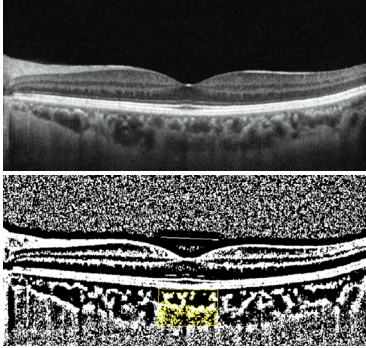
The Thai Journal of Ophthalmology

ปีที่ 39 ฉบับที่ 2 กรกฎาคม-ธันวาคม 2568

สารบัญ

- 91 รายงานผู้ป่วย: ก้อนอักเสบเรื้อรังสีเหลืองบริเวณเบ้าตาในผู้ใหญ่
ปพิชญา เต็มภัทราโชค, พ.บ.
มงคล อุยประเสริฐกุล, พ.บ.
สุนิสา สิ้นธวงค์, พ.บ.
- 97 อาการแสดงจำเพาะทางตาที่นำไปสู่การวินิจฉัยโรคท้าวแสนปมชนิดที่สองชนิดเกิดเร็ว
พิทยา ภมรเวชวรรณ, พ.บ.
สุนงกช ศุภีรสกุล, พ.บ.
รวี จงพิพัฒน์ชัย, พ.บ.
ศุภิตดา เจียมสวัสดิ์, พ.บ.

Contents



ภาพปก Enhanced-depth optical coherence tomography central B-scan of the left eye (left panel). Following binarization, the choroid was divided into dark (vascular lumen) and bright (stroma) pixels. A region of interest (highlighted in yellow) with a width of 1,500 μm centered on the foveal center was selected to compute the choroidal vascularity index (CVI).

#Unpaired t-test for continuous data and Chi-square test for categorical data

ix Editor's Note

Original Articles

61 Choroidal Vascularity Index Changes after Treatment of Persistent Central Serous Chorioretinopathy with either Spironolactone or Half-Dose Photodynamic Therapy

Wongsiri Taweebanjongsin, MD

Sitthipol Piriyaakontorn, MD

Karntida Chanwimol, MD

Julaporn Pooliam, MD

Rupesh Agrawal, MD

Srinivas R Sadda, MD

75 Effects of Dexamethasone Implant on Contralateral Central Foveal and Subfoveal Choroidal Thickness in Unilateral Uveitic Macular Edema

Mukaddes Damla Ciftci, MD

Mine Esen Baris, MD

Suzan Guven, MD

Case Reports

83 Acute Unilateral Isolated Ptosis as a Complication of Frontal Sinusitis: A Case Report

Busayanut Puangsricharoen, MD



จักษุเวชสาร

The Thai Journal of Ophthalmology

Vol. 39 No. 2 July-December 2025

Contents

91 Adult Orbital Xanthogranuloma: A Case Report

Paphitchaya Temphattharachok, MD

Monkol Uiprasertkul, MD

Sunisa Sintuwong, MD, MPPM, MSc

97 Specific Ocular Findings Leading to the Diagnosis of Early-Onset Neurofibromatosis

Type 2

Pittaya Phamonvaechavan, MD

Subongkoch Subhadhirasakul MD

Rawi Jongpipatchai, MD

Supathida Jiamsawad, MD

Choroidal Vasculature Index Changes after Treatment of Persistent Central Serous Chorioretinopathy with either Spironolactone or Half-Dose Photodynamic Therapy

Wongsiri Taweebanjongsin, MD¹⁻³ Sitthipol Piriyakootorn, MD¹, Karntida Chanwimol, MD¹
Julaporn Pooliam, MD⁴, Rupesh Agrawal, MD⁵⁻⁸, Srinivas R Sadda, MD^{2,3}

Abstract

Purpose: To evaluate choroidal vasculature index (CVI) changes after treatment with either spironolactone or half-dose photodynamic therapy (PDT).

Design: Retrospective study

Methods: We enrolled 34 patients with subretinal fluid accumulation persisting for more than 3 months due to central serous chorioretinopathy (CSC); 16 patients were treated with spironolactone and 18 with PDT. We reviewed the central OCT-B scans at baseline and 1 and 3 months after treatment. We defined the CVI as the percent of vascular/luminal pixels over the total number of pixels and compared the results between the treatment groups.

Results: The baseline CVIs were 60.33% in the spironolactone treatment group and 60.51% in the PDT group. After treatment, the CVI remained similar in the spironolactone group, but it increased significantly one month (63.35%) and three months (63.56%, $P = 0.004$, 0.001) after the PDT. The total and luminal choroidal areas were both decreased after PDT, but only the stromal area was significantly decreased at one and three months ($P = 0.001$ and $P < 0.001$, respectively). By month three, the subfoveal choroidal thickness (SFCT) had decreased by $30.32 \mu\text{m}$ ($P = 0.013$) in the PDT group and by $18.88 \mu\text{m}$ ($P = 0.195$) in the spironolactone group.

Conclusion: After CSC treatment, the choroid remained virtually unchanged following the spironolactone therapy, whereas the choroidal thickness was significantly reduced and the CVI increased following PDT. These anatomic changes in the choroid following PDT may explain why the effects of PDT are more durable and potent than those of spironolactone for CSC.

Keywords: central serous chorioretinopathy (CSC), choroidal vasculature index (CVI), choroidal thickness (CT), choroidal vasculature, spironolactone, half-dosed photodynamic therapy

¹Department of Ophthalmology, Mettapracharak Hospital, Nakhon Pathom, Thailand

²Doheny Image Reading Center, University of California-Los Angeles (UCLA), Los Angeles, California, United States

³Department of Ophthalmology, Stein Eye Institute, UCLA, Los Angeles, United States

⁴Research Group and Research Network Division Research Department, Faculty of Medicine Siriraj Hospital, Bangkok, Thailand

⁵Department of Ophthalmology, Tan Tock Seng Hospital, NHG Eye Institute, Singapore

⁶Singapore Eye Research Institute, Singapore

⁷Moorfields Eye Hospital, NHS Foundation Trust, London, United Kingdom

⁸Lee Kong Chian School of Medicine, Nanyang Technological University, Singapore

Introduction

Central serous chorioretinopathy (CSC) is a pachychoroid spectrum disorder¹⁻⁴ characterized by choroidal abnormalities including increased choroidal thickness, large dilated outer choroidal vessels that may compress the inner choroid⁴, and choroidal vascular hyperpermeability⁵⁻⁷ (best detected via indocyanine green angiography imaging)⁸⁻¹⁰. Subretinal fluid accumulation may occur during periods of activity and persisting fluid can lead to vision loss.

The etiology and pathogenesis of CSC remain unclear; however, corticosteroids (exogenous or endogenous) seem to aggravate the condition¹¹⁻¹⁵; and, over- or inappropriate activation of the mineralocorticoid receptor (MR)⁷ may lead to choroidal vascular dilatation and hyperpermeability. MR activation may also promote muscle cell fibrosis via activation of the placental growth factor (PGF)/VEGF receptor 1 (VEGFR1) pathway, and MR antagonists may prevent pathologic vascular remodeling¹⁶. Zhao and colleagues found mineralocorticoid receptors in ganglion, cells of inner nuclear layer, and Muller cells in rats eyes¹⁷. Spironolactone is a well-established MR antagonist used to treat hypertension and congestive heart failure, and it has been suggested as a potential oral treatment for non-resolving CSC¹⁸⁻²⁴. Small studies have reported potential treatment efficacies in patients with chronic CSC¹⁸⁻²³ as well as faster absorption of subretinal fluid in cases of acute CSC²⁴. Lee and colleagues found similar short-term efficacies of best-corrected visual acuity improvement and decrease of subretinal fluid height for both oral spironolactone and half-dose photodynamic therapy²³, but only patients in the PDT group decreased their subfoveal choroidal thickness after the treatment. Whether the choroidal thickness changes following MR antagonist treatment remains a controversial point^{17,19-21}. Eplerenone is another MR antagonist that may be preferable for male patients with CSC because it is less probable to induce hormonal

issues like gynecomastia. However, eplerenone's MR antagonist effect is considerably less potent than spironolactone's. Moreover, eplerenone failed to demonstrate a significant treatment benefit in eyes with CSC in a randomized clinical trial²⁵.

Photodynamic therapy (PDT) has been well-studied and is commonly accepted as an effective treatment for chronic CSC²⁶⁻²⁹. PDT is typically applied using either half-dose (of verteporfin) or half-fluence (of light) regimens. PDT's effects are thought to be due to a reduction in choroidal hyperpermeability²⁹ through transient occlusion of choriocapillaris, a histopathological finding demonstrated in human eyes³⁰. This inner choroidal occlusion is also responsible for the subsequent decrease in choroidal thickness and choroidal vascular dilatation³¹⁻³².

The choroidal vascularity index (CVI) is a metric developed to specifically assess the relative proportions of the vasculature and stroma in the choroid³³⁻³⁹, the index is valuable for assessing the status of various diseases, providing information not captured by measurements of choroidal thickness alone. The CVI is computed as the ratio of the luminal area (LA) divided by the total choroidal area (TCA). A difference in CVI suggests a difference in the proportion of vessels relative to that in the stroma. The CVI in eyes with active CSC has been shown to be higher than that in the fellow eyes when compared to those in age-matched controls³⁴. Kinoshita and colleagues reported that both the hyperreflective area (stromal structure) of the inner choroid and the hyporeflexive area (luminal structure) of the outer choroid are decreased significantly after half-dose PDT in patients with CSC⁴⁰. However, to the best of our knowledge, no studies have assessed the impact of oral spironolactone on the CVI. Thus, we designed this study to evaluate the CVI changes over time following oral spironolactone in both the affected CSC eye and the fellow eye, and we compared the effects to those after half-dose PDT.

Methods

For this retrospective study, we identified and reviewed the records of 34 consecutive patients who were newly diagnosed and recurrent CSC with persistent subretinal fluid for more than 3 months at the Mettapracharak Hospital between 2013 and 2018. Among these patients, 16 (16 eyes) received 50 mg per day of oral spironolactone (Aldactone; Pfizer, New York, NY) for 30 days and 18 patients (18 eyes) were treated with half-dose PDT (HD-PDT). Our inclusion criteria included: (1) age between 18 years old and above; and, (2) best-corrected visual acuity (BCVA) between 20/200 and 20/30. Both unilateral and bilateral CSC were included in the study. We excluded records of patients with any of the following criteria: any evidence of other macular disease or a complicating feature such as choroidal neovascularization, polypoidal choroidal vasculopathy, or diabetic macular edema; and, pregnant patients. The Medical Ethics Committee of Mettapracharak Hospital approved the research protocols, the number of approval was COA011/2563, and we conducted the research adhering to the tenets set forth in the Declaration of Helsinki.

The patients in the PDT group had all undergone fluorescein angiography (FA) (HRA-2; Heidelberg Retina Angiograph System, Heidelberg Engineering, Heidelberg, Germany) to identify the leakage region (fluid on OCT) and to calculate the treatment spot size (defined as the smallest circular region able to completely cover the region of leakage on the FA). After obtaining informed consents, 3 mg/m² of verteporfin (Visudyne; Novartis AG, Bulach, Switzerland) were infused in the antecuboidal vein during a period of 10 minutes; subsequently, 5 minutes after the infusion, the leakage area was treated with 683 nm of light for a period of 83 seconds, with a total irradiation of 50 J/cm². Following the PDT, patients were advised to avoid bright lights or sunlight for at least 24 hours.

The records of all patients also included data

on duration of symptoms (months), defined as the recognition of disturbance of visual function, including visual acuity, color vision and contrast sensitivity⁵ and a complete ophthalmic examination including BCVA, slit-lamp biomicroscopy, dilated ophthalmoscopy, and spectral domain optical coherence tomography (OCT) with enhanced-depth imaging (EDI) OCT (Spectralis; Heidelberg Engineering, Heidelberg, Germany) at baseline just prior to treatment, and again 1 and 3 months after treatment. The main outcome endpoints for our study were the change in CVI and the subfoveal choroidal thickness (SFCT) 1 and 3 months after the start of treatment (PDT or spironolactone).

To facilitate evaluation of the choroid, the spectral domain OCT (Spectralis, Heidelberg Engineering, Heidelberg, Germany) scans were acquired using the EDI technique. A 30 × 15 degrees (8.8 × 4.4 mm) pattern centered on the fovea was scanned consisting of 19 B-scans with a spacing of 238 μm between scans. Each B-scan was averaged 9 to 11 times. The central B-scan was used to measure the choroidal thickness and CVI. The subfoveal choroidal thickness (SFCT) was manually measured from the retinal pigment epithelium (RPE) outer surface to the inner scleral surface using the caliper tool in the Heidelberg Eye Explorer Software (Version 1.10.4.0). We defined the central subfield thickness (CST) as the average thickness of the macula in the 1-mm central region of the Early Treatment of Diabetic Retinopathy Study (ETDRS) grid, and we measured it from the internal limiting membrane to the RPE; therefore, it included both the intraretinal thickening and subretinal fluid.

Choroidal Vascularity Index (CVI) Computation

We selected the central EDI-OCT B-scan for binarization using the publicly-available Image J software (Fiji; <http://fiji.sc/Fiji>). We computed the binarization protocol from Agrawal and colleagues³⁵. First, we selected the region of interest (ROI) as a zone

on the foveal center with a width of 1,500 μm (750 μm to the nasal and temporal sides of the fovea). We placed the inner border of the ROI at the outer RPE and the outer border at the choroid-sclera interface. The images were adjusted to 8 bits, and we applied the Niblack autocal threshold method (Figure 1) to differentiate pixels into bright and dark ones. We counted dark pixels as belonging to the LA corresponding to the vascular lumens. The remaining bright pixels were deemed to represent the choroidal stroma. Before the

computation, we compared the binarized image with the original structural OCT image to confirm that the binarized image accurately reflected the vascular and stromal components visible on the original OCT image. The total number of pixels in the ROI served as the denominator for CVI computations. We defined the CVI as the ratio of the LA divided by the total area. An experienced, certified Doheny Image Reading Center (DIRC) grader (WT) performed all gradings and the CVI analyses.

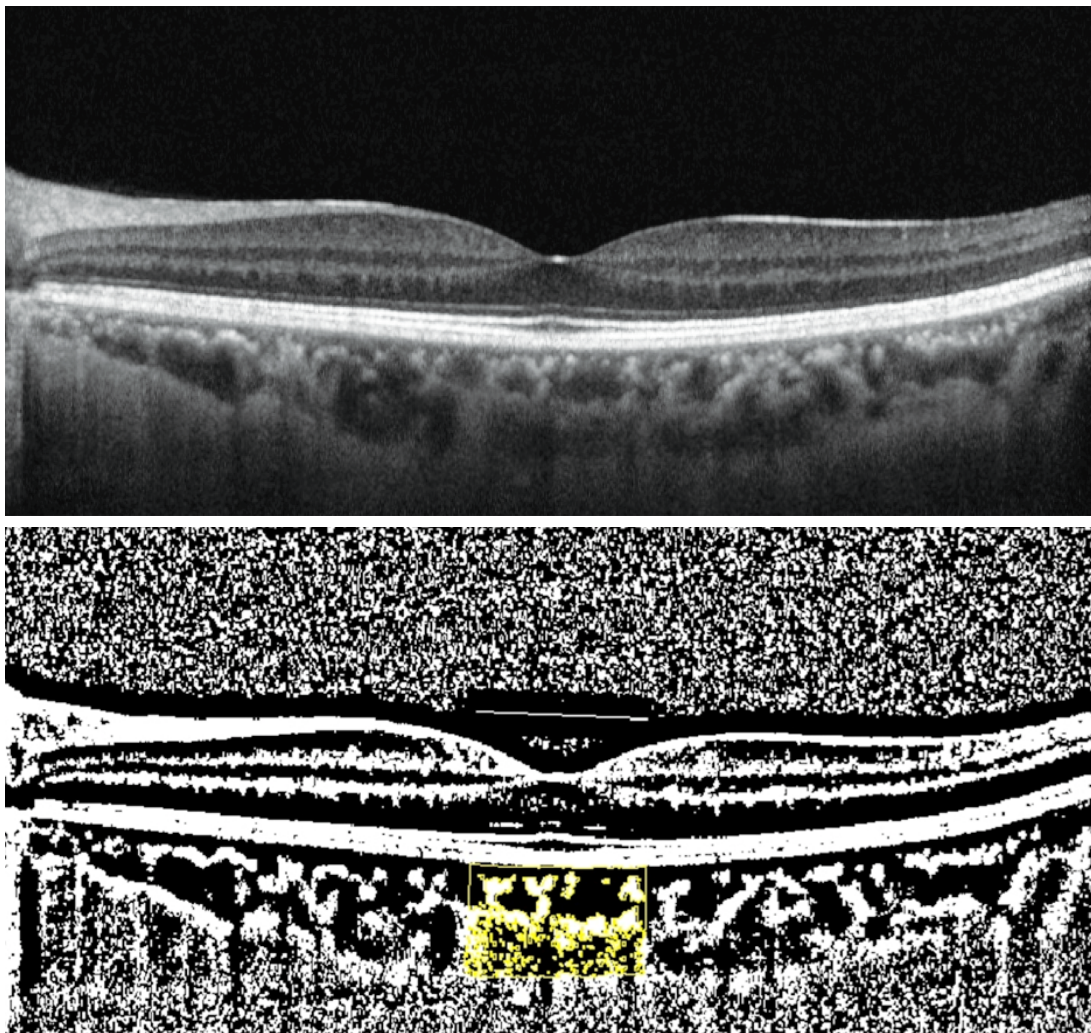


Figure 1 Enhanced-depth optical coherence tomography central B-scan of the left eye (left panel). Following binarization, the choroid was divided into dark (vascular lumen) and bright (stroma) pixels. A region of interest (highlighted in yellow) with a width of 1,500 μm centered on the foveal center was selected to compute the choroidal vascularity index (CVI). #Unpaired t-test for continuous data and Chi-square test for categorical data

Statistical Analysis

All assessments were performed in both the study and the fellow eyes. We analyzed all data using SPSS version 21.0 (SPSS, Chicago, IL). Descriptive data (age, sex, duration of symptom) are presented as means \pm SDs. Baseline characteristics were used Unpaired *t*-test for continuous data and Chi-square test for categorical data. We analyzed pairwise comparisons of data (BCVA, CST, SFCT, CVI, the total choroidal area, and the luminal and stromal areas) between baseline and 1- and 3-month values using repeated ANOVA measures with Bonferroni correction. We applied unpaired *t*-tests to compare means between the study groups and between baseline and follow-up values within groups and paired *t*-test to compare between study eyes and fellow eyes. We considered *P* values < 0.05 as indicative of statistical significance.

Results

Our study included records of 34 patients: 16 patients (16 eyes) in the spironolactone (SPRL) group and 18 patients (18 eyes) in the PDT group. The baseline characteristics of the two groups were similar (Table 1); 3 patients in the PDT group had prior steroid use, whereas none of the patients in the spironolactone group had been prescribed steroids before. In addition, the groups were well balanced in terms of age (mean age \pm SD, 50.13 \pm 11.41 years in the spironolactone group, 49.17 \pm 8.90 years in the PDT group; *P* = 0.785), proportions of women:men (2:14 and 1:17; *P* = 0.591), duration of symptoms (7.44 months and 7.67 months; *P* = 0.868), and baseline BCVAs (0.48 and 0.40 logMAR; *P* = 0.391).

Table 1 Demographic data

Demographic data	Spironolactone (N = 16)	PDT (N = 18)	<i>P</i>
Mean age \pm SD (years)	50.13 \pm 11.41	49.47 \pm 8.75	0.785
Sex: male (%)	14 (87.5)	17 (94.4)	0.597
Underlying disease (%)			
Hypertension	3 (18.8)	8 (44.4)	0.152
Diabetes	2 (12.5)	2 (11.1)	1.000
Dyslipidemia	1 (6.3)	3 (16.7)	0.604
Smoking (%)	4 (25.0)	4 (22.2)	1.000
Insomnia (%)	4 (25.0)	1 (5.6)	0.164
Stress (%)	5 (31.3)	3 (16.7)	0.429
History of corticosteroid use (%)	0 (0.0)	3 (16.7)	0.230
Duration of symptom (months)	7.44 \pm 4.50	7.67 \pm 3.45	0.868

#Unpaired *t*-test for continuous data and Chi-square test for categorical data

Choroidal vascularity index (CVI), and total choroidal, luminal, and stromal areas

The baseline CVIs were 60.33% in the spironolactone group and 60.51% in the PDT group ($P = 0.894$). After treatment, the CVIs increased slightly (not statistically significant) to 61.72% and 61.28% at 1 and 3 months, respectively, in the spironolactone group. However, in the PDT group, the CVIs increased significantly to 63.35% ($P = 0.004$) at the 1-month follow-up and to 63.56% ($P = 0.001$) at the 3-month follow-up (Table 2).

The total choroidal areas at baseline were 2.25 mm² in the spironolactone group and 2.18 mm² in the PDT group, but only the PDT group showed a statistically significant decrease ($P = 0.016$ at month 1 follow-up, $P = 0.019$ at 3-month follow-up). This was primarily due to a reduction in stromal area in the PDT group from 0.87 mm² at baseline to 0.75 mm² at the 1-month follow-up ($P = 0.001$) and to 0.74 mm² at the 3-month follow-up ($P \leq 0.001$). The luminal areas did not change significantly in either group (Table 2).

Subfoveal choroidal thickness (SFCT)

The mean subfoveal choroidal thickness (SFCT) at baseline in the eyes with active CSC (study eyes; SE) tended to be thicker than those in the fellow eyes (FE), although the differences only reached statistical significance in the PDT group ($P = 0.031$). After treatment, the SFCTs in the study eyes decreased significantly from 397.13 μm to 359.88 μm at the 1-month follow-up ($P \leq 0.001$) and to 366.81 μm (P

$= 0.013$) at the 3-month follow-up in the PDT group. However, in the spironolactone group, the SFCT reduction was not statistically significant, dropping from 430.94 μm at baseline to 417.94 μm at the 1-month follow-up ($P = 0.237$) and to 412.06 μm at the 3-month follow-up ($P = 0.195$; Table 2). The SFCTs in the fellow unaffected eyes remained similar in all groups (Table 2).

Central subfield thickness (CST)

In the spironolactone group, the mean CSTs decreased from 364.25 μm at baseline to 342.56 μm at the 1-month follow-up ($P = 1.000$) and to 273.31 μm at the 3-month follow-up ($P = 0.042$). In the PDT group, the mean CSTs decreased from 387.71 μm at baseline to 251.18 μm ($P = 0.002$) at the 1-month follow-up and remained at that level (254.00 μm) at the 3-month follow-up ($P \leq 0.001$; Table 2). By the 3-month follow-up, residual subretinal fluid was apparent in 50% of spironolactone eyes and in 33.33% of PDT eyes.

Best-corrected visual acuity (BCVA)

The mean visual acuities improved significantly at the 3-month follow-up in both groups, going from 0.48 LogMAR at baseline to 0.27 LogMAR in the spironolactone group ($P = 0.001$), and from 0.40 LogMAR to 0.23 LogMAR in the PDT group ($P = 0.006$; Table 2).

In the unaffected fellow eyes, the choroidal markers remained similar over time in both groups (Table 2).

Table 2 Impact of oral spironolactone or half-dose PDT in eyes with persistent CSC and in unaffected fellow eyes

	Spironolactone group				PDT group				<i>P</i> [#]	
	Study eyes (n = 16)	<i>P</i> [#]	Fellow eyes (n = 12)	<i>P</i> [#]	Study eyes (n = 18)	<i>P</i> [#]	Fellow eyes (n = 17)	<i>P</i> [#]		
CVI (%)										
Baseline	60.33 ± 3.97		64.26 ± 2.79		60.51 ± 3.59		62.64 ± 4.39		0.894	
1-month follow-up	61.72 ± 3.31	0.319	64.66 ± 4.31	1.000	63.35 ± 4.00	0.004	63.23 ± 3.65	1.000	0.227	
3-month follow-up	61.28 ± 3.98	0.627	64.56 ± 3.37	1.000	63.56 ± 3.56	0.001	63.74 ± 3.74	0.545	0.102	
Total choroidal area (mm²)										
Baseline	2.25 ± 0.55		1.85 ± 0.33		2.18 ± 0.40		1.86 ± 0.55		0.711	
1-month follow-up	2.19 ± 0.56	1.000	1.83 ± 0.39	1.000	2.01 ± 0.48	0.016	1.82 ± 0.55	0.934	0.342	
3-month follow-up	2.20 ± 0.61	1.000	1.88 ± 0.41	1.000	2.00 ± 0.53	0.019	1.79 ± 0.51	0.282	0.336	
Luminal area (mm²)										
Baseline	1.34 ± 0.27		1.18 ± 0.18		1.31 ± 0.20		1.15 ± 0.30		0.747	
1-month follow-up	1.34 ± 0.29	1.000	1.18 ± 0.20	1.000	1.26 ± 0.25	0.511	1.14 ± 0.29	1.000	0.427	
3-month follow-up	1.33 ± 0.31	1.000	1.20 ± 0.22	1.000	1.26 ± 0.29	0.537	1.12 ± 0.27	0.912	0.503	
Stromal area (mm²)										
Baseline	0.91 ± 0.29		0.67 ± 0.16		0.87 ± 0.21		0.71 ± 0.27		0.696	
1-month follow-up	0.85 ± 0.27	0.266	0.66 ± 0.21	1.000	0.75 ± 0.24	0.001	0.68 ± 0.27	1.000	0.281	
3-month follow-up	0.87 ± 0.31	0.645	0.68 ± 0.20	1.000	0.74 ± 0.26	<0.001	0.66 ± 0.25	0.299	0.220	
SFCT (μm)										
Baseline	430.94 ± 98.48		351.10 ± 68.60		397.13 ± 70.80		329.13 ± 103.45		0.274	
1-month follow-up	417.94 ± 98.16	0.237	348.30 ± 66.88	1.000	359.88 ± 82.56	<0.001	318.67 ± 104.93	0.160	0.080	
3-month follow-up	412.06 ± 102.57	0.195	336.30 ± 77.58	0.464	366.81 ± 93.35	0.013	313.80 ± 104.30	0.224	0.202	
CST (μm)										
Baseline	364.25 ± 95.27				387.71 ± 177.52				0.643	
1-month follow-up	342.56 ± 98.32	1.000			251.18 ± 56.04	0.002			0.002	
3-month follow-up	273.31 ± 84.34	0.042			254.00 ± 64.29	<0.001			0.463	
BCVA (LogMAR)										
Baseline	0.48 ± 0.26				0.40 ± 0.29				0.391	
1-month follow-up	0.38 ± 0.22	0.274			0.30 ± 0.30	0.192			0.353	
3-month follow-up	0.27 ± 0.16	0.001			0.23 ± 0.26	0.006			0.598	

P[#] significance level between baseline and follow-up values.

P^{*} significance level of difference between spironolactone and PDT groups.

Discussion

In this study on the treatment outcomes for eyes with CSC and persistent subretinal fluid, we observed significant differences between eyes treated with oral spironolactone and those treated with half-dose PDT. PDT was associated with a more rapid reduction in central subfield thickness (and resolution of subretinal fluid) and a more profound and rapid reduction in choroidal thickness. Interestingly, the stromal area (but not the luminal area) decreased over time after the treatment, particularly in the PDT group. This preferential reduction in the stromal component was reflected in the mean CVI, which showed an increase in the PDT group following treatment.

CVI is a relatively recent measure, although an extensive body of literature already mentions its potential application in the context of various diseases. For example, Agarwal and colleagues proposed CVI as a potentially useful marker to monitor panuveitis progression³⁵ and Vogt-Koyanagi-Harada disease (VKH).³⁶ Notably, baseline CVIs were higher in the panuveitis and VKH eyes compared to those in the normal controls, a finding that may indicate the presence of blood flow stasis in the choroid due to the inflammatory process. The CVIs decreased after the treatment. In studies on age-related macular degeneration (AMD) Xin Wei and colleagues³⁸ reported that the mean CVI in exudative AMD eyes was lower than that in the non-neovascular fellow eye due to a reduction in the luminal area. In another study of eyes with non-neovascular AMD without reticular pseudodrusen (RPD), the CVI was found to be lower in eyes with RPD than in normal control eyes.³⁹ These initial studies suggested that the CVI, along with the stromal and luminal areas, may be useful markers for monitoring changes in the vascular or stromal choroidal components.

Although the pathophysiology of CSC is unclear, the dilated vessels observed commonly in the outer

choroid (Haller's layer) indicate that choroidal congestion may be pervasive. Given the prominence of these large vessels, one would presume that vessel engorgement and vascular volume increments should contribute to an increased CVI. Indeed, Agrawal and colleagues reported that the CVIs in CSC eyes were higher than in age-matched healthy eyes, and appeared to parallel the greater subfoveal choroidal thickness (SFCT) in the same eyes³⁴. In recent study of short term CVI change after PDT, Bazvand and colleagues found central macular thickness and CVI decreased after 6 weeks of PDT laser which explained that the mechanism of PDT in CSC disease is the recovery of choriocapillaris circulation⁴¹. In a similar manner, it would be reasonable to hypothesize that the thinning of the choroid that is observed with successful treatments (particularly after PDT), is driven by a reduction in the area of the engorged outer choroidal vessels. In our study, the luminal area decreased following PDT, but the reduction was not statistically significant. Instead, we found that the key driver of initial choroidal thinning following PDT was a statistically significant reduction in the stromal area at the 1-month follow-up. This greater reduction in the stromal area relative to that in the vascular area is reflected in the CVI increase following treatment. The pathophysiologic importance of the larger pre-treatment stromal area is emphasized by the fact that in both the spironolactone and PDT groups, the stromal area was larger in the study eyes than in unaffected fellow eyes. Given the presumed importance of the choroidal vasculature and hyperpermeability for the CSC pathophysiology, what is the function of the stroma in the pathophysiology? One hypothesis posits that the choroidal vascular changes can lead to an increase in hydrostatic pressure and a diffuse swelling of the choroidal stroma. Indeed, this may be the substrate for the large patches of hyperfluorescence that are commonly seen on indocyanine green angiography images in these

patients. Sonoda and colleagues reported a larger hyperreflective area in the inner choroid, and they speculated that it was related to inflammation and edema of the choroidal stroma present in the setting of active CSC⁴². Chan and colleagues suggested that the main PDT action mechanism reduces this choroidal hyperpermeability²⁹.

Our study revealed a difference in the anatomic response to PDT and spironolactone. Whether the SFCT changes following spironolactone treatment is a controversial point^{17,19-21,23}. For example, there were no SFCT changes after 3 months of spironolactone treatment in a study by Lee and colleagues²³ or after 1 year of treatment with spironolactone or eplerenone in another study by Ghadiali and colleagues¹⁹. By contrast, Zhao and colleagues observed a decrease 2 weeks after therapy initiation¹⁷, Bousquet and colleagues showed a significant decrease after 1 month²⁰, and Durich and colleagues found a reduction in choroidal thickness in a recalcitrant CSC patient after 6 months of oral spironolactone or eplerenone²¹. In addition, skepticism over the potential therapeutic impact of mineralocorticoid antagonists has increased after a randomized trial of eplerenone failed to show efficacy for treating CSC. However, spironolactone is a more potent antagonist than eplerenone, and it should be ideally evaluated in a similar randomized trial. Regardless of the apparently contradictory evidence, in our study, we observed little impact of spironolactone on the total choroidal, luminal, and stromal areas or CVIs. The SFCT decreased slightly over the 3 months of follow-up, but the reduction was not statistically significant. Despite this, we did observe a significant reduction in the CST (and subretinal fluid) and an vision improvement by the 3-month follow-up in the patients treated with spironolactone— the reduction in CST, however, was slower than that in the patients treated with PDT, who showed a dramatic reduction

by the 1-month follow-up. Taken together, our findings suggest that, any impact of mineralocorticoid antagonists operate via different mechanisms that do not significantly involve the choroid, unlike the mechanisms of PDT.

Our study is not without limitations and these must be considered when interpreting our findings: First, our study was retrospective in nature and we cannot rule out ascertainment bias or unknown imbalances between the study arms. However, we are fortunate because all the participants were imaged using the same protocol. Second, our follow-up lengths were relatively short at three months. As a result, we were not able to detect long-term differences in the treatment arms in terms of visual acuity, recurrent disease activity, or further choroidal changes. Third, our sample size was relatively small. Although we observed significant differences in CVI and stromal area in the PDT arms, we were likely underpowered to detect smaller differences due to treatment effect, particularly in the spironolactone arm. However, this was a pilot study to evaluate CVI changes following treatment, and our findings can guide the design of future, large, prospective longitudinal studies. Finally, although the CVI computation methodology we used, based on binarization, has been well-established in the literature, the lack of histological assessments for comparison introduces uncertainty regarding the accuracy of classifying pixels as representing stromal tissue.

In summary, in this pilot study of CVI analysis after spironolactone and PDT therapy for CSC, we found that the CVI increased after PDT, but not after spironolactone treatment. Moreover, the CVI change was primarily driven by a reduction in stromal area. If confirmed in larger, prospective studies, these findings may provide new insights into the pathophysiology of CSC and response to therapy.

Acknowledgments/Discloure

Funding/Support: None

Financial Disclosures:

Drs. Taweebanjongsin, Piriya-koon-torn, Chanwimol, Pooliam and Agrawal report no conflicts. Dr. Satta reports personal fees from Allergan, personal fees from Amgen, personal fees from Bayer, personal fees from Novartis, personal fees from Roche/Genentech, personal fees from 4DMT, personal fees and non-financial support from Optos, personal fees and non-financial support from Heidelberg, personal fees and non-financial support from Centervue, personal fees and non-financial support from Nidek, non-financial support from Carl Zeiss Meditec, non-financial support from Tocpon, during the conduct of the study.

References

1. Warrow DJ, Hoang QV, Freund KB. Pachychoroid pigment epitheliopathy. *Retina* 2013;33:1659-72.
2. Gallego-Pinazo R, Dolzo-Marco R, Gómez-Ulla MS, Freund KB. Pachychoroid disease of macula. *Retina. Med Hypo Discov Innov Ophthalmol* 2014;3.
3. Phasukkijwatana N, Freund KB, Dolzo-Marco R, et al. Peripapillary pachychoroid syndrome. *Retina* 2017;0:1-16.
4. Cheung CMG, Lee WK, Koizumi H, Dansingani K, Lai TYY, Freund KB. Pachychoroid disease. *Eye* 2019;33:14-33.
5. Nicholson B, Noble J, Forooghian F, Meyerle C. Central serous chorioretinopathy: update on pathophysiology and treatment. *Surv Ophthalmol* 2013;58:103-26.
6. Prünke C, Flammer J. Choroidal capillary and venous congestion in central serous chorioretinopathy. *Am J Ophthalmol* 1996;121:26-34.
7. Daruich A, Matet A, Dirani A, Bousquet E, Zhao M, Farman N, Jaisser F, Behar-Cohen F. Central serous chorioretinopathy: recent findings and new physiopathology hypothesis. *Retin Eye Res* 2015; 48:82-118.
8. Spaide RF, Hall L, Haas A, Campeas L, Yannuzzi LA, Fisher YL, Guyer DR, Slakter JS, Sorenson JA, Orlock DA. Indocyanine green videoangiography of older patients with central serous chorioretinopathy. *Retina* 1996;16:203-13.
9. Hayashi K, Hasegawa Y, Tokoro T. Indocyanine green angiography of central serous chorioretinopathy. *Int Ophthalmol* 1986;9:37-41.
10. Guyer DR, Yanuzzi LA, Slakter JS, Sorenson JA, Ho A, Orlock D. Digital indocyanine green angiography of central serous chorioretinopathy. *Arch Ophthalmol* 1994;112:1057-62.
11. Tittl MK, Spaide RF, Wong D, Pilotto E, Yannuzzi LA, Fisher YL, Freund B, Guyer DR, Slakter JS, Sorenson JA. Systemic findings associated with central serous chorioretinopathy. *Am J Ophthalmol* 1999;128:63-68.
12. Haimovici R, Gragoudas ES, Duker JS, Sjaarda RN, Elliott D. Central serous chorioretinopathy associated with inhaled or intranasal corticosteroids. *Ophthalmology* 1997;104:1653-60.
13. Iida T, Spaide RF, Negrao SG, Carvalho CA, Yannuzzi LA. Central serous chorioretinopathy after epidural corticosteroid injection. *Am J Ophthalmol* 2001;132:423-5.
14. Hurvitz AP, Hodapp KL, Jadgechew J, Solomon DJ, Stollendorf HS, Provencher MT. Central serous chorioretinopathy resulting in altered vision and color perception after glenohumeral corticosteroid injection. *Orthopedics* 2009;32.
15. Ezra N, Taban M, Behroozan D. Central serous chorioretinopathy associated with topical corticosteroids in a patient with psoriasis. *J Drugs Dermatol* 2011;10:918-21.
16. McGraw AP, Bagley J, Chen WS, Galayda C, Nickerson H, Armani A, Caprio M, Carmeliet P, Jaffe IZ. Aldosterone increases early atherosclerosis and promotes plaque inflammation through a placental growth factor-dependent mechanism. *J Am Heart Assoc* 2013;2:e000018.
17. Zhao M, Célérier I, Bousquet E et al. Mineralocorticoid receptor is involved in rat and human ocular chorioretinopathy. *J Clin Invest* 2012;122:2672-9.
18. Herold TR, Prause K, Wolf A, Mayer WJ, Ulbig

- MW. Spironolactone in treatment of central serous chorioretinopathy a case series. *Graefes Arch Clin Exp Ophthalmol* 2014;252:1985-91.
19. Ghadiali Q, Jung JJ, Yu S, Patel SN, Yannuzzi LA. Central serous chorioretinopathy treated with mineralocorticoid antagonists: a one-year pilot study. *Retina* 2016;36:611-8.
 20. Bousquet E, Beydoun T, Rothschild PR, et al. Spironolactone for nonresolving central serous chorioretinopathy: a randomized controlled crossover study. *Retina* 2015;35:2505-15.
 21. Daruich A, Matet A, Dirani A, Gallice M, Nicholson L, Sivaprasad S, Behar-Cohen F. Oral mineralocorticoid receptor antagonists: real-life experience in clinical subtypes of nonresolving central serous chorioretinopathy with chronic epitheliopathy. *Trans Vis Sci Tech* 2016;5:2.
 22. Herold TR, Rist K, Priglinger SG, Ulbig MW, Wolf A. Long-term results and recurrence rates after spironolactone treatment in non-resolving central serous chorio-retinopathy (CSCR). *Graefes Arch Clin Exp Ophthalmol* 2017;255:221-9.
 23. Lee JH, Lee SC, Kim H, Lee CS. Comparison of short-term efficacy between oral spironolactone treatment and photodynamic therapy for the treatment of nonresolving central serous chorioretinopathy. *Retina* 2017;0:1-7.
 24. Sun X, Shuai Yuanlu, Fang Wangyi, Jia Li, Weizhong Ge, Songtao Yuan, Qinghuai Liu. Spironolactone versus observation in the treatment of acute central serous chorioretinopathy. *Br J Ophthalmol* 2018;102:1060-5.
 25. Lotery A, Sivaprasad S, O'Connell A, et al. Eplerenone for chronic central serous chorioretinopathy in patients with active, previous untreated disease for more than 4 months(VICI): a randomized, double-blind, placebo-controlled trial. *Lancet* 2020;395:294-303.
 26. Nicolò M, Zoli D, Musolino M, Traverso CE. Association between the efficacy of half-dose photodynamic therapy with indocyanine green angiography and optical coherence tomography findings in the treatment of central serous chorioretinopathy. *Am J Ophthalmol* 2012;153:474-480.e1.
 27. Ober MD, Yannuzzi LA, Do DV, Spaide RF, Bressler NM, Jampol LM, Angelilli A, Eandi CM, Lyon AT. Photodynamic therapy for focal retinal pigment epithelial leaks secondary to central serous chorioretinopathy. *Ophthalmology* 2005;112:2088-94.
 28. Sakalar YB, Keklikci U, Unlu K, Alakus MF, Kara IH. Effects of photodynamic therapy with verteporfin for the treatment of chronic central serous chorioretinopathy: an uncontrolled, open-label, observation study. *Curr Ther Res Clin Exp* 2010;71:173-85.
 29. Chan WM, Lam DS, Lai TY, Tam BS, Liu DT, Chan CK. Choroidal vascular remodeling in central serous chorioretinopathy after indocyanine green guided photodynamic therapy with verteporfin: a novel treatment at a primary disease level. *Br J Ophthalmol* 2003;87:1453-8.
 30. Schimdt-Erfurth U, Laqua H, Schlötzer-Schrehard U, Viestenz A, Naumann GO. Histopathological changes following photodynamic therapy in human eyes. *Arch Ophthalmol* 2002;120:835-44.
 31. Izumi T, Koizumi H, Maruko I, Takahashi Y, Sonoda S, Sakamoto T, Iida T. Structural analyses of choroidal after half-dose verteporfin photodynamic therapy for central serous chorioretinopathy. *Br J Ophthalmol* 2016;0:1-5.
 32. Maruko I, Iida T, Sugano Y, Ojima A, Ogasawara M, Spaide RF. Subfoveal choroidal thickness after treatment of central serous chorioretinopathy. *Ophthalmology* 2010;117:1792-9.
 33. Agrawal R, Gupta P, Tan K-A, Cheung CMG, Wong TY, Cheng C-Y. Choroidal vascularity index as a measure of vascular status of the choroid: measurements in healthy eyes from a population-based study. *Sci Rep* 2016;6:21090.
 34. Agrawal R, Chhablani J, Tan K-A, Shah S, Sarviya C, Banker A. Choroidal vascularity index in central serous chorioretinopathy. *Retina* 2016;0:1-6.
 35. Agrawal R, Salman M, Tan K-A, Karampelas M, Sim DA, Keane PA, Pavesio C. Choroidal vascularity index (CVI) – A novel optical coherence tomography parameter for monitoring patients with panuveitis? *PLOS ONE* 2016;11:e0146344. doi:10.1371/journal.pone.0146344.
 36. Agrawal R, Li LKH, Nakhate V, Khandelwal N,

- Mahendradas P. Choroidal vascularity index in Vogt-Koyanagi-Harada disease progression. *Trans Vis Sci Tech* 2016;5:7. doi:10.1167/tvst.5.4.7.
37. Koh LHL, Agrawal R, Khandelwal N, Sai Charan LS, Chhablani J. Choroidal vascular changes in age-related macular degeneration. *Acta Ophthalmol* 2017;95:e597-e601.
38. Wei X, Ting DSW, Ng YW, Khandelwal N, Agrawal R, Cheung CMG. Choroidal vascularity index A novel optical coherence tomography based parameter in patients with exudative age-related macular degeneration. *Retina* 2016;0:1-6.
39. Velaga SB, Nittala MG, Vupparaboina KK, Jana S, Chhablani J, Haines J, Pericak-Vance MA, Stambolian D, Sadda SR. Choroidal vascularity index and choroidal thickness in eyes with reticular pseudodrusen. *Retina* 2019;00:1-6.
40. Kinoshita T, Mitamura Y, Mori T, Akaiwa K, Semba K, Egawa M, Mori J, Sonoda S, Sakamoto T. Changes in choroidal structures in eyes with chronic central serous chorioretinopathy after half-dose photodynamic therapy. *PLOS ONE* 2016;11:e0163104. doi:10.1371/journal.pone.0163104.
41. Fatemeh Bazvand, Hassan Asadigandomani, Alireza Nezameslami, Reza Sadeghi, Mahdi Soleymanzadeh, Alireza Khodabande and Hamid Riazi-Esfahani. Short term choroidal microvascular changes following photodynamic therapy in chronic central serous chorioretinopathy. *Photodiagnosis Photodyn Ther*. 2023 Dec;44:103807. doi: 10.1016/j.pdpdt.2023.103807. Epub 2023 Sep 20.
42. Sonoda S, Sakamoto T, Kuroiwa N, Arimura N, Kawano H, Yoshihara N, Yamashita T, Uchino E, Kinoshita T, Mitamura Y. Structural changes of inner and outer choroid in central serous chorioretinopathy determined by optical coherence tomography. *PLOS ONE* 2016;11:e0157190. doi:10.1371/journal.pone.0157190.

การศึกษาการเปลี่ยนแปลงของ choroidal vascularity index ในการรักษาโรคจุดภาพชัดแยกชั้นจากรั่วรั่วเรื้อรังด้วยสไปโรโนแลคโตนเปรียบเทียบกับการรักษาด้วย photodynamic therapy



Wongsiri Taweebanjongsin, MD¹⁻³

วงศ์ศิริ ทวีบรรจงสิน, พ.บ.

Julaporn Pooliam, MD⁴

จุฬารภรณ์ พูลเอี่ยม, พ.บ.

Sitthipol Piriyaakontorn, MD¹

สิทธิพล พิริยคุณธร, พ.บ.

Rupesh Agrawal, MD⁵⁻⁸

Karntida Chanwimol, MD¹

กาญจน์ธิดา จันทน์วิมล, พ.บ.

Srinivas R Sadda, MD^{2,3}

บทคัดย่อ:

วัตถุประสงค์ของงานวิจัย: โรคจุดภาพชัดรั่วน้ำ (Central Serous Chorioretinopathy: CSC) ปัจจุบันพบว่าเป็นโรคที่มีความผิดปกติของชั้นคอร์รอยด์ โดยจะพบชั้นคอร์รอยด์หนาตัวขึ้น (Increased choroidal thickness) และเส้นเลือดในชั้นคอร์รอยด์มีการขยายตัวขึ้น (Dilated choroidal vessels) การวัดชั้นคอร์รอยด์ด้วยวิธี CVI (Choroidal vascular index) เป็นวิธีการวัดที่จะประเมินเส้นเลือดในชั้นคอร์รอยด์กับชั้นเนื้อเยื่อคอร์รอยด์ (choroidal stroma) ทำให้เห็นได้ว่า มีความผิดปกติที่ส่วนใดเป็นหลักการรักษาโรคจุดภาพชัดรั่วน้ำด้วยวิธีเลเซอร์ Photodynamic therapy (PDT) และ Spironolactone ที่มีคุณสมบัติเป็น Mineralocorticoid antagonist เป็นหนึ่งในวิธีที่นำมาใช้ในการรักษาโรคจุดภาพชัดรั่วน้ำ โดยวัตถุประสงค์ในการศึกษานี้เพื่อดูการเปลี่ยนแปลงของชั้นคอร์รอยด์ โดยจะประเมินการเปลี่ยนแปลงของเส้นเลือดคอร์รอยด์และชั้นเนื้อเยื่อคอร์รอยด์ก่อนและหลังการรักษาด้วย Half-dose PDT และ spironolactone

รูปแบบการวิจัย: การศึกษาย้อนหลัง

วิธีการศึกษา: choroidal vascularity index (CVI) เป็นการศึกษาชั้นคอร์รอยด์ โดยนำภาพตัดขวางจอตา (Optical coherence tomography) มาวิเคราะห์หัดส่วนของ vascular/luminal pixels เทียบกับ total number of pixels โดยนำมาคิดเป็นเปอร์เซ็นต์ โดยการศึกษานี้ นำผู้ป่วยที่ได้รับการวินิจฉัยว่าเป็นโรคจุดภาพชัดแยกชั้นจากรั่วรั่วเรื้อรังที่ได้รับการรักษาด้วยสไปโรโนแลคโตนจำนวน 16 ราย และ photodynamic therapy จำนวน 18 ราย มาเปรียบเทียบการเปลี่ยนแปลงของ CVI หลังได้รับการรักษาที่ 1 และ 3 เดือนตามลำดับ

ผลการศึกษา: พบว่ากลุ่มที่ได้รับสไปโรโนแลคโตนไม่มีการเปลี่ยนแปลงของ CVI ,กลุ่มที่ได้รับ photodynamic therapy มีการเปลี่ยนแปลงของ CVI ที่ 1 และ 3 เดือนอย่างมีนัยสำคัญทางสถิติ (60.51% เทียบกับ 63.35% และ 63.56% $P = 0.004, 0.001$) และพบว่าความหนาของชั้นคอร์รอยด์หลังได้รับการรักษาที่ 3 เดือนลดลง $30.32 \mu\text{m}$ ($P = 0.013$) ในกลุ่มที่ได้รับ photodynamic therapy เทียบกับ $18.88 \mu\text{m}$ ($P = 0.195$) ในกลุ่มสไปโรโนแลคโตน

สรุป: จากการศึกษาการรักษาด้วยสไปโรโนแลคโตนไม่พบการเปลี่ยนแปลงของชั้นคอร์รอยด์ ในขณะที่การรักษาด้วย photodynamic therapy มีความหนาของชั้นคอร์รอยด์ลดลงและ CVI เพิ่มขึ้นอย่างมีนัยสำคัญทางสถิติ ดังนั้นการรักษาด้วย photodynamic therapy ส่งผลต่อการเปลี่ยนแปลงทางกายวิภาคของชั้นคอร์รอยด์มากกว่าสไปโรโนแลคโตน ซึ่งอาจส่งผลให้ประสิทธิภาพของการรักษาด้วย photodynamic therapy มีประสิทธิภาพมากกว่าสไปโรโนแลคโตน

คำสำคัญ: โรคจุดภาพชัดแยกชั้นจากรั่วรั่ว, สไปโรโนแลคโตน

Footnotes and Financial Disclosures

Financial Support: None

Originally receive: 19/9/2024

Final revision: 6/10/2025

Accepted: 11/10/2025

Conflict of interest:

Dr. Satta reports honoraria from Amgen, Bayer, Genentech/Roche, Novartis, Allergan, 4DMT, Heidelberg, Optos, Nidek, and Centervue.

Drs. Taweebanjongsin, Piriyakootorn, Chanwimol, Pooliam and Agrawal have no conflicts of interest to report.

Synopsis

The choroidal vascular index, reflecting the choroidal vascular status, changed significantly after photodynamic therapy, but remained virtually unchanged following spironolactone therapy in eyes with central serous chorioretinopathy.

Correspondence to: Srinivas R Satta, 1355 San Pablo Street DVRC 211, Los Angeles, CA, 90033, USA.

Tel: +1 562 202 8889 / Fax: +1 323 342 6460 / Email: ssatta@doheny.org

Effects of Dexamethasone Implant on Contralateral Central Foveal and Subfoveal Choroidal Thickness in Unilateral Uveitic Macular Edema

Mukaddes Damla Ciftci, MD¹, Mine Esen Baris, MD², Suzan Guven, MD²

Abstract

Objectives: To investigate the effect of intravitreal dexamethasone implant application on retinal and choroidal thickness of contralateral eye of the patients with uveitic macular edema.

Materials and Methods: This study included 17 patients with non-infectious uveitic macular edema treated with intravitreal dexamethasone implantation. The central foveal thickness (CFT) and subfoveal choroidal thickness (SFCT) measurement taken by swept-source optical coherence tomography were evaluated retrospectively at the pre- and post-injection 1st, 3rd, 6th months, and its relationship with visual acuity was investigated.

Results: Four (23.5%) of the patients had intermediate, 3 (17.6%) had anterior and 10 (58.8%) of them had panuveitis. The mean CFT and SFCT of the eyes with intravitreal implants were 494.3 ± 171.1 and 346.1 ± 68.8 μm respectively. A statistically significant reduction in CFT was observed at the 1st (318.1 ± 65.0 , $p < 0.001$), 3rd (314.2 ± 74.2 , $p < 0.001$), and 6th (320.6 ± 77.1 , $p < 0.001$) months following intravitreal injection. There was a statistically significant decrease of SFCT from the baseline in the 1st month (203.9 ± 62.1 μm , $p < 0.001$), 3rd month (222.1 ± 61.6 μm , $p = 0.002$) and 6th month (224.3 ± 72.6 μm , $p = 0.023$) after the injection. The mean CFT of contralateral eyes was 205.8 ± 55.0 μm before injection and did not change significantly post-injection. The mean SFCT of the contralateral eyes before the injection was 311.2 ± 72.9 μm . Decrease in SFCT of the contralateral eyes at 1st month (288.6 ± 68.5 μm) ($p = 0.02$) was statistically significant. No significant change was observed in visual acuity after injection in contralateral eyes.

Conclusion: Decrease in the choroidal thickness of the contralateral eyes of patients was so limited and temporary that they did not reflect on their visual acuity. Therefore, it was thought that this may be secondary to the small amount of systemic absorption of intravitreal dexamethasone.

Keywords: choroidal thickness, dexamethasone implant, uveitic macular edema

¹University of Health Sciences, Diskapi Yildirim Beyazit Training and Research Hospital, Ankara, Turkiye

²Ege University Faculty of Medicine, Department of Ophthalmology, Izmir, Turkiye

Introduction

Uveitic macular edema (UME) is a prominent cause of vision loss in patients with uveitis. It is defined as fluid accumulation in the form of cystoid spaces or diffuse retinal thickening within the retinal layers or in the subretinal area due to disruption of the blood-retinal barrier (BRB) because of ocular inflammation.¹ Although it can be observed in all forms of uveitis, it most often accompanies posterior uveitis.² Corticosteroids contribute significantly to anatomical and functional recovery in most cases of non-infectious uveitis complicated by macular edema by their immunosuppressive and anti-inflammatory effects.³ Even though the deterioration of the BRB primarily plays a role in the development of macular edema. Enhanced depth imaging optical coherence tomography; (EDI-OCT) and swept-source optical coherence tomography (SS-OCT) technologies have shown that the choroid also has a place in the pathophysiology and can be used in the evaluation of treatment response, allowing for more detailed imaging of the choroid.^{4,5} There are case reports suggesting that the application of dexamethasone intravitreal implant (Ozurdex[®]; Allergan, Inc., Irvine, CA) may also have an anti-inflammatory effect on the contralateral eye in patients with uveitis.⁶ This observation raises the possibility that intravitreally administered dexamethasone may be systemically absorbed. Such a consideration is important both for monitoring the contralateral eye and for assessing potential systemic effects.

The aim of this study is to evaluate and present the effect of intravitreal dexamethasone implant application on retinal and choroidal thickness in the contralateral eye of patients and its relationship with visual acuity in the treatment of UME.

Materials and Methods

A retrospective chart review was performed in the uvea department of Ege University Hospital, Ophthalmology Department. Data from 17 patients who underwent intravitreal dexamethasone implant for non-infectious UME between January 2021 and March 2022 were reviewed. All injections were carried out by two experienced ophthalmic surgeons (MEB and SG). Central foveal thickness (CFT) and subfoveal choroidal thickness (SFCT) measurements of treated and contralateral eyes before injection and 1st, 3rd and 6th months after injection were analyzed retrospectively and their relationship with visual acuity was investigated. CFT and SFCT measurements were evaluated on SS-OCT (DRI-OCT1 Atlantis system, Topcon) images. All participants were scanned by the same experienced OCT technician. SS-OCT imaging was performed using the device's automated macular scan mode, and B-scan segmentation was generated from 50 cross-sectional images. Eyes with low image quality (signal strength <7) were not included in the analysis. All measurements of CFT and SFCT were made by two individual graders (MDC and MEB), who were not masked, at different times using the same image, and the average value was used.

The patients aged ≥ 18 years who had unilateral macular edema and non-infectious inactive uveitis under systemic immunosuppressive therapy were included in the study. Inactivity criteria were based on laser flare photometry measurements below 7.5 and the absence of cells in the anterior chamber for anterior uveitis. For intermediate and panuveitis, in addition to these, the absence of vitritis and the absence of leakage on fluorescein angiography were accepted as inactivity criteria. In the enrolled patients, persistent UME, despite the absence of clinically detectable

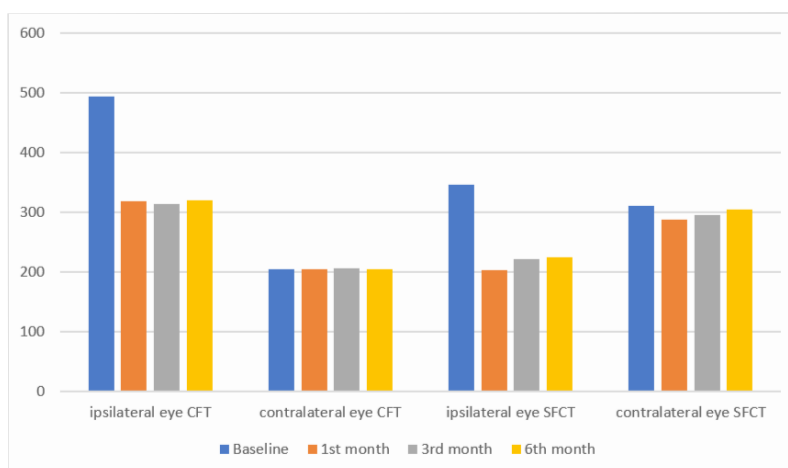
active cellular inflammation, may be attributable to chronic structural or vascular alterations, or to ongoing subclinical inflammatory activity.⁷ Consecutive patients who met the aforementioned criteria and underwent intravitreal implantation between January 2021 and March 2022 were included in the study.

Patients with additional systemic pathology or ophthalmological disease that may cause inflammation were excluded from the study. Additionally, patients with systemic comorbidities known to potentially affect the integrity of the blood–retinal barrier as BRB (including diabetes mellitus, hypertension, chronic kidney disease, and other metabolic disorders) were excluded from the study.

SPSS 26.0 (IBM Corporation, Armonk, New York, United States) and PAST 3 (Hammer, Ø., Harper, D.A.T., Ryan, P.D. 2001. Paleontological statistics) programs were used in the analysis of the variables. The Shapiro–Wilk test was used to assess the normality of the data distribution. Changes in CMT and SFCT values over time were evaluated using repeated-measures ANOVA within the General Linear Model framework. This study was approved by the Institutional Ethics Review Board of Ege University, Turkey with approval number of 22-12.2T/19 and conducted in agreement with the tenets of the Helsinki Declaration. Each participant signed a written informed consent form for the use of their medical data.

Results

The female/male ratio of 17 patients with a mean age of 56.8 ± 15.1 years was 14/3. The baseline mean CFT and SFCT of the eyes with intravitreal implants were 494.3 ± 171.1 and 346.1 ± 68.8 μm , respectively. A statistically significant reduction in CFT was observed at the 1st (318.1 ± 65.0 , $p < 0.001$), 3rd (314.2 ± 74.2 , $p < 0.001$), and 6th (320.6 ± 77.1 , $p < 0.001$) months following intravitreal injection. There was a statistically significant decrease of SFCT from the baseline in the 1st month (203.9 ± 62.1 μm , $p < 0.001$), 3rd month (222.1 ± 61.6 μm , $p = 0.002$) and 6th month (224.3 ± 72.6 μm , $p = 0.023$) after the injection. The mean CFT of contralateral eyes was 205.8 ± 55.0 μm before injection and did not change significantly at 1st month (204.7 ± 62.2 μm), 3rd month (206.4 ± 57.8 μm) and 6th month (204.5 ± 73.4 μm) ($p = 0.95$). The baseline SFCT of the contralateral eyes before the injection was 311.2 ± 72.9 μm . There was statistically significant decrease in SFCT of the contralateral eyes at 1st month (288.6 ± 68.5 μm) ($p = 0.02$). A mean decrease of 26.82 μm (95% CI: -41.40 to -12.24 μm) in SFCT thickness was observed at post-injection 1st month. SFCT measurements of the contralateral eyes did not change significantly from the baseline value at 3rd month (295.2 ± 77.2 μm) ($p = 0.1$) and 6th month (304.1 ± 77.5 μm) ($p = 0.3$) after injection. Graphic 1 shows change of CFT and SFCT measurements of ipsilateral and contralateral eyes.



Graphic 1 Change of CFT and SFCT measurements of ipsilateral and contralateral eyes at baseline, 1st, 3rd and 6th month after intravitreal Ozurdex® implantation

Intraocular pressure (IOP) was found to be significantly higher at the 1st month (17.1 ± 2.9 mmHg) compared to the baseline (13.7 ± 2.7 mmHg) in the eyes with dexamethasone implant ($p < 0.001$). During the 6-month follow-up, ocular hypertension controlled with anti-glaucomatous eye drops was observed in 3 eyes (17.6%) that had received an intravitreal implant. In contralateral eyes, there was no significant difference in intraocular pressure compared to the baseline (14.4 ± 2.2 mmHg) at 1st month (15.1 ± 2.3 mmHg) ($p = 0.18$). No other adverse events were observed and no serious complications were encountered.

The median best corrected visual acuity (BCVA) before the procedure and at 1st month in the injected eyes were 0.7 (0.2-1.8) and 0.5 (0.1-1.8) logMAR, respectively, with a statistically significant increase ($p = 0.003$). Additionally, the mean decimal BCVA increased from 0.22 ± 0.18 before injection to $0.33 \pm$

0.25 after injection, representing a mean improvement of 0.11 ± 0.13 . This change was statistically significant ($p = 0.003$; 95% CI, 0.041–0.178). No significant correlation was found between visual gains and change in CFT value after injection in eyes treated with dexamethasone implant ($p = 0.49$; $r = 0.13$). On the other hand, there was no significant difference in the median BCVA of the contralateral eyes before the injection 0.2 (0-1.3) and 1st month after the injection 0.2 (0-1) ($p = 0.85$). The mean decimal BCVA of the contralateral eyes slightly decreased from 0.67 ± 0.34 before injection to 0.67 ± 0.31 after injection, with a mean change of -0.006 ± 0.13 . This difference was not statistically significant ($p = 0.85$; 95% CI, -0.074 to 0.062).

Table 1 includes the demographic and clinical characteristics of patients.

Table 1 Clinical and demographic features of the patients

Patient No.	Age/Gender	Diagnosis	Laterality of UME	Systemic Treatment	Baseline Demographic and Clinical Characteristics				Outcome Data			
					Baseline BCVA (logMAR)		Baseline SFCT (µm)		Post-injection 1 st month BCVA (logMAR)		Post-injection SFCT (µm)	
					Ipsilat.	Contralat.	Ipsilat.	Contralat.	Ipsilat.	Contralat.	Ipsilat.	Contralat.
1	53/F	Intermediate uveitis	L	Methotrexate (15 mg/week)	1.8	0	325	299	1.8	0	303	274
2	44/F	Intermediate uveitis	L	Azathioprine (100 mg/day)	0.7	0	480	468	0.5	0	436	400
3	58/F	Panuveitis (Behçet's disease)	L	Adalimumab (40 mg/2 weeks), methylprednisolone (8 mg/day)	0.7	0.2	300	348	0.7	0.2	253	369
4	58/F	Panuveitis	R	Adalimumab (40 mg/2 weeks)	0.2	0.7	369	253	0.1	0.3	354	212
5	72/F	Panuveitis	R	Cyclosporine (100 mg/day)	0.5	0	381	307	0.2	0.1	375	297
6	72/F	Panuveitis	R	Azathioprine (100 mg/day)	0.8	0.2	358	340	0.2	0.1	317	300
7	69/F	Anterior uveitis	L	Methylprednisolone (8 mg/day)	1	1.3	405	378	0.7	0.8	363	298
8	53/F	Intermediate uveitis	L	Methotrexate (15 mg/week)	1.3	0	325	289	1.3	0	307	273
9	57/F	Panuveitis (Behçet's disease)	R	Azathioprine (50 mg/day), methylprednisolone (8 mg/day)	1.3	1	331	323	1	1	323	299
10	68/F	Anterior uveitis	R	Methylprednisolone (8 mg/day)	1.3	0.3	340	285	1	0.3	327	284
11	20/M	Panuveitis (Behçet's disease)	R	Adalimumab (40 mg/2 weeks)	0.3	0	388	316	0.2	0	357	245
12	68/F	Anterior uveitis	L	Methylprednisolone (8mg/day)	1	0.2	320	272	1	0.2	290	272
13	33/F	Panuveitis	R	Adalimumab (40 mg/2 weeks), methotrexate (15 mg/week)	0.7	0.3	389	372	0.5	0.4	318	325
14	44/M	Panuveitis (Behçet's disease)	L	Azathioprine (50 mg/day), olchicine (1 mg/day)	0.4	0	404	394	0.4	0	389	360
15	53/F	Panuveitis (Sarcoidosis)	R	Methotrexate (15 mg/week)	1	0	273	266	0.7	0	226	247
16	67/F	Panuveitis	R	Cyclosporine (100 mg/day)	0.5	0.4	229	244	0.5	0.5	312	240
17	77/M	Intermediate uveitis	L	Azathioprine (100 mg/day)	0.4	0.1	156	137	0.2	0.3	155	140

BCVA: Best-corrected visual acuity, F: female, M: male, Ipsilat.: ipsilateral, Contralat.: contralateral, R: right, L: left, UME: uveitic macular edema

Discussion

In this retrospective study, which included 17 cases of inactive non-infectious uveitis who underwent dexamethasone implant for macular edema, a limited decrease was found in the mean SFCT value in the contralateral eyes at the 1st month after the injection, which was not reflected in the visual acuity. Chang-Lin et al.⁸ demonstrated the pharmacokinetic and pharmacodynamic properties of the dexamethasone implant and showed that the drug is present in low concentrations in plasma until the 90th day after intravitreal administration. Especially in the uveitic patients, increased vascular permeability and impaired BRB may increase the systemic absorption of dexamethasone. Habet-Wilner et al.⁶ reported bilateral improvement after unilateral intravitreal dexamethasone implantation in a 26-year-old uveitis patient with bilateral vitritis and macular edema. As the patients included in the present study showed no evidence of active cellular inflammation, the effect of the dexamethasone implant was assessed exclusively on UME.

In a retrospective study including the contralateral eyes of 13 patients and 14 control subjects who were administered intravitreal dexamethasone for cystoid macular edema, no significant difference was found between the two groups in terms of central macular thickness and visual acuity.⁹ Systemic absorption of intravitreal medications may vary from patient to patient and in different disease groups such as diabetes, retinal vein occlusion and uveitis, depending on the degree of deterioration in the BRB.^{10,11}

Gulati et al.¹² reported bilateral good anatomical and functional outcomes in a patient with radiation maculopathy refractory to bevacizumab treatment after intravitreal dexamethasone implant administration. In the case report, it was stated that the patient underwent 4 intravitreal dexamethasone implant applications and

after the last injection, there was improvement in vision and a decrease in macular thickness in the contralateral eye. In our study, all the patients that included had only 1 dexamethasone implantation between January 2021 and March 2022. The difference between the number of intravitreal applications may explain the lack of statistically significant change in visual acuity in the contralateral eyes in the present study. On the other hand, the fact that only unilateral macular edema was present in the patients that included the study may also be the reason for this situation.

Significant limitations of the current study are retrospective nature of the chart review design, short follow-up time, absence of systemic dexamethasone plasma level measurements, and limited number of the patients. Furthermore, the lack of a control group or a comparative group with non-uveitic cystoid macular edema constitutes another limitation of the present study. The fact that patients included in our study were under systemic immunosuppressive therapy and did not exhibit active cellular inflammation allowed us to specifically UME; however, the potential influence of immunosuppressive treatment on choroidal and retinal thickness constitutes a potential confounding factor influencing the study outcomes. Choroidal thickness is known to show diurnal variation, and the absence of time-of-day standardization in our measurements constitutes a potential confounding factor that may have affected the study outcomes.¹³

Conclusion

Intravitreal dexamethasone implant is an effective option in the treatment of UME. In this particular study, it provides a decrease in CFT and SFCT values in the eyes that were treated with dexamethasone implant 1, 3 and 6 months after the application. In the contralateral eyes, a decrease in choroidal thickness was observed in the first month after injection and it was thought

that this effect, which was limited and temporary, not reflected on visual acuity, may be secondary to a small amount of systemic absorption of dexamethasone. The transient decrease observed in SFCT can be considered clinically insignificant. Owing to the retrospective design and small sample size, the present results are preliminary and warrant confirmation in larger prospective studies.

Future studies with larger sample sizes and systemic pharmacokinetic monitoring are warranted to better assess the potential effects of the dexamethasone implant on the contralateral eye.

References

1. Sood G, Patel BC. Uveitic Macular Edema. In: StatPearls. Treasure Island (FL): StatPearls Publishing; May 24, 2022.
2. Rothova A, Suttorp-van Schulten MS, Frits Treffers W, Kijlstra A. Causes and frequency of blindness in patients with intraocular inflammatory disease. *Br J Ophthalmol.* 1996;80(4):332-6.
3. Lowder C, Belfort R, Lightman S, et al. Dexamethasone intravitreal implant for noninfectious intermediate or posterior uveitis. *Arch Ophthalmol.* 2011;129(5):545-50.
4. Campos A, Campos EJ, Martins J, et al. Viewing the choroid: where we stand, challenges and contradictions in diabetic retinopathy and diabetic macular oedema. *Acta Ophthalmol* 2017;95:446-59.
5. Zur D, Iglicki M, Busch C, et al. OCT biomarkers as functional outcome predictors in diabetic macular edema treated with dexamethasone implant. *Ophthalmology* 2018;125:267-75.
6. Habot-Wilner Z, Sorkin N, Goldenberg D, Goldstein M. Bilateral effect of unilateral dexamethasone intravitreal implant in a case of noninfectious uveitic macular edema and vitritis. *Retin Cases Brief Rep.* 2015;9(2):151-3.
7. Tomkins-Netzer O, Lightman S, Drye L, et al. Outcome of treatment of uveitic macular edema: The multicenter uveitis steroid treatment trial 2-year results. *Ophthalmology.* 2015;122(11):2351-9.
8. Chang-Lin JE, Attar M, Acheampong AA, et al. Pharmacokinetics and pharmacodynamics of a sustained-release dexamethasone intravitreal implant. *Invest Ophthalmol Vis Sci.* 2011;52:80-6.
9. Fleissig E, Sigford DK. Effect of Extended Release Steroid Implants on the Contralateral Eye. *BMC Ophthalmol.* 2022;22(1):131. Published 2022 Mar 22.
10. Klaassen I, Van Noorden CJ, Schlingemann RO. Molecular basis of the inner blood-retinal barrier and its breakdown in diabetic macular edema and other pathological conditions. *Prog Retin Eye Res.* 2013;34:19-48.
11. Chahal PS, Fallon TJ, Kohner EM. Measurement of Blood-Retinal Barrier Function in Central Retinal Vein Occlusion. *Arch Ophthalmol.* 1986;104(4):554-7.
12. Gulati SK, Pillai GS, Radhakrishnan N. Effect of intravitreal dexamethasone implant on the contralateral eye in recalcitrant radiation maculopathy. *Oman J Ophthalmol.* 2019;12(2):129-32.
13. Jiang X, Xiao P, Tan Q, Zhu Y. Variation of choroidal thickness during the waking period over three consecutive days in different degrees of myopia and emmetropia using optical coherence tomography. *PeerJ.* 2023;11:e15317.

Effects of Dexamethasone Implant on Contralateral Central Foveal and Subfoveal Choroidal Thickness in Unilateral Uveitic Macular Edema



Mukaddes Damla Ciftci, MD¹



Mine Esen Baris, MD²



Suzan Guven, MD²

¹University of Health Sciences, Diskapi Yildirim Beyazit Training and Research Hospital, Ankara, Turkiye

²Ege University Faculty of Medicine, Department of Ophthalmology, Izmir, Turkiye

Footnotes and Financial Disclosures

Financial Support: None

Originally receive: 22/1/2025

Final revision: 16/10/2025

Accepted: 8/11/2025

Funding:

The authors received no financial support for the research, authorship and publication of this article.

Declaration of Interest:

The authors declare that there is no conflict of interest.

Ethical Approval:

This study was approved by the Institutional Ethics Review Board of Ege University, Turkey with approval number of 22-12.2T/19 and conducted in agreement with the tenets of the Helsinki Declaration. Each participant signed a written informed consent form for the use of their medical data.

Correspondence to: Mukaddes Damla Ciftci, MD

University of Health Sciences, Diskapi Yildirim Beyazit Training and Research Hospital, Ankara, Turkiye

Phone: 90 543 827 85 05

e-mail: mdamlac@gmail.com

Acute Unilateral Isolated Ptosis as a Complication of Frontal Sinusitis: A Case Report

Busayanut Puangricharoen, MD

Abstract

Objective: Acquired upper-eyelid ptosis can be traumatic, mechanical, neurogenic, or myogenic in origin. However, oculomotor nerve or cranial nerve (CN) III palsy caused by frontal sinusitis is extremely rare. The purpose of this report is to document an unusual case of frontal sinusitis in a 15-year-old boy with acute unilateral ptosis as the sole presenting sign of CN III palsy.

Case report: A 15-year-old Thai boy presented with a 2-day history of left-sided upper-eyelid ptosis preceded by a 1-week history of influenza A infection. His pupils were equivalent in size bilaterally, and extraocular muscles exhibited full motility. Magnetic resonance imaging of the brain and orbit revealed fluid opacification and mucosal thickening, predominantly in the left frontal sinus, with no levator palpebrae superioris abnormalities. The case was diagnosed as frontal sinusitis associated with CN III palsy. The ptosis had completely resolved by the fifth day of intravenous levofloxacin.

Conclusions: Frontal sinusitis can lead to palsy of the superior branch of CN III presenting with only isolated ptosis. This case highlights a potential complication of acute sinusitis and raises awareness of a rare differential diagnosis in isolated, unilateral ptosis. Diagnostic neuroimaging may assist in managing such atypical cases.

Keywords: cranial nerve (CN) III palsy, oculomotor nerve palsy, pediatric, ptosis, sinusitis

Introduction

Upper-eyelid ptosis can be congenital or acquired, and it can be traumatic, mechanical, neurogenic, or myogenic in origin.¹ Aponeurotic ptosis due to levator dehiscence has been most commonly recorded in older people, whereas congenital ptosis, oculomotor nerve or cranial nerve (CN) III palsy, Horner's syndrome, and mechanical ptosis have been widely described in pediatric populations.^{1,2} However, it is extremely rare for CN III palsy to cause acute unilateral isolated ptosis without limited extraocular muscle motility, afferent pupillary defect, or other neuro-ophthalmological findings. A previous report described that acute ptosis associated with isolated CN III palsy occurred in less than 1% of sphenoid sinusitis cases.³ This is even rarer in frontal sinusitis, as just one patient with CN III palsy presenting with only isolated ptosis caused by frontal sinusitis has been reported.⁴

The objective of this case report is to highlight an unusual case of frontal sinusitis in a pediatric patient with acute unilateral ptosis as the sole presenting feature of isolated oculomotor nerve or CN III palsy.

Case Presentation

A 15-year-old boy with no past medical or ocular history presented to an ophthalmology clinic in Bangkok, Thailand with a 2-day history of left-sided unilateral isolated ptosis that appeared when he had woken up. He had a 1-week history of low-grade fever, mild frontal headache, and minimal nasal discharge. He had been diagnosed with influenza A infection, for which oseltamivir was prescribed for 5 days. He did not complain of any visual impairment, diplopia, fluctuating ptosis, or orbital pain. He also ruled out any history of trauma, recent vaccination, or treatment of

the upper face via injection of botulinum toxin.

Analysis of the vital signs revealed a temperature of 37.1°C, blood pressure of 114/68 mmHg, pulse of 80 beats per minute, and respiratory rate of 20 breaths per minute, with oxygen saturation of 99%. No abnormal head posture or facial anhidrosis was noted. Upon external ophthalmic examination, no periorbital swelling, redness or warmth, or mechanical cause of ptosis was observed; however, there was mild tenderness over the left eyebrow.

His best-corrected visual acuity was 20/25 in both eyes. The intraocular pressure as determined by rebound tonometry was 16 and 19 mmHg in the right and left eyes, respectively. The pupils were reactive to light and equivalent in size bilaterally in bright and dim light, without relative afferent pupillary defect. No remarkable findings of anterior and posterior segments were made upon slit lamp examination. He had partial left upper-eyelid ptosis with the presence of a normal lid crease (Figure 1). The distance from the corneal light reflex to the central upper-eyelid margin, known as margin-reflex distance 1, in the right eye was 3 mm, while in the left it was -2 mm. The vertical palpebral fissure was 8 mm on the right and 3 mm on the left. Levator function was symmetrical and measured 15 mm bilaterally. There were negative findings for all typical myasthenia gravis lid signs, including the fatigability test, Cogan's lid twitch, the curtain sign, and the peek sign. Negativity for Marcus Gunn jaw-winking was also confirmed. Extraocular muscles exhibited full motility in all fields of gaze (Figure 2). Both eyes were orthophoric, and an alternate cover-uncover test did not reveal a phoria. The visual fields were full to confrontation bilaterally. Other cranial nerves revealed no remarkable findings.



Figure 1 Photograph of the patient. The patient at initial presentation with left upper-eyelid ptosis.

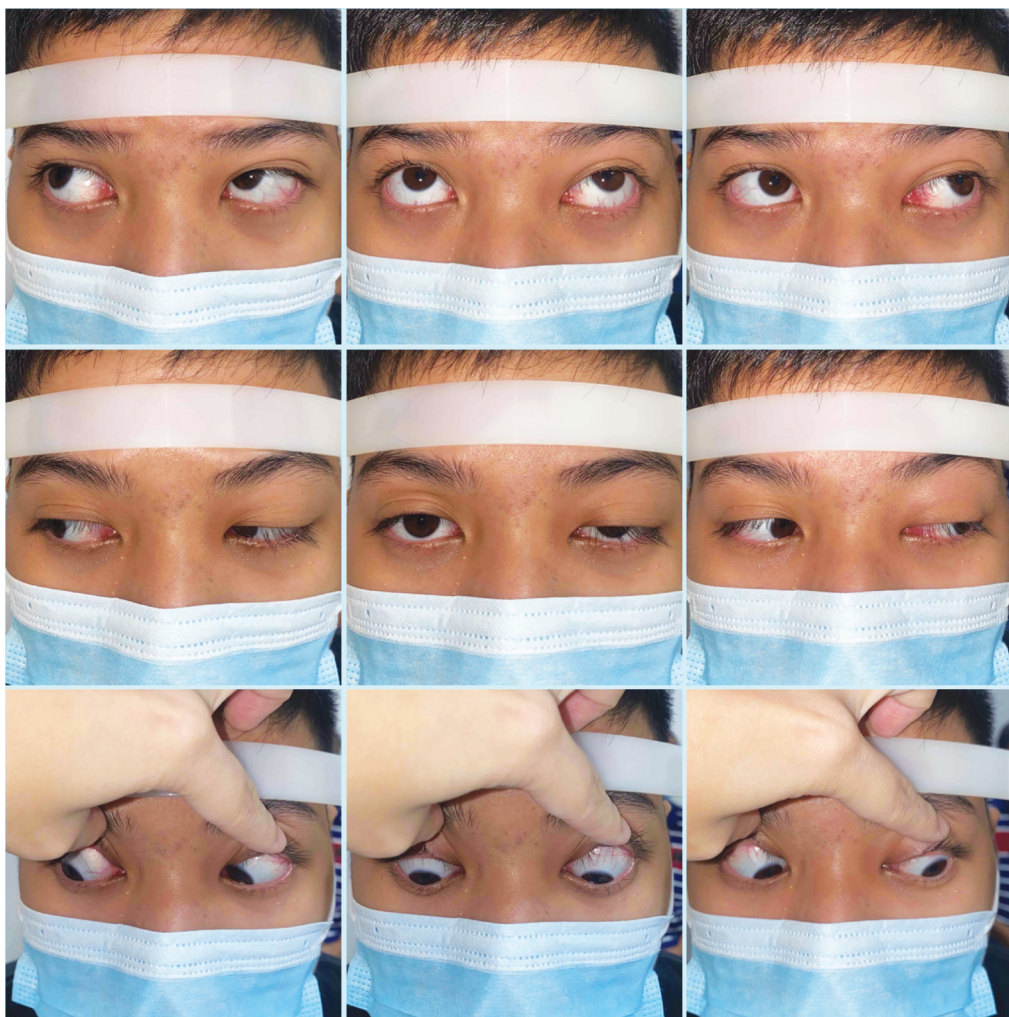


Figure 2 Photographs of the patient. The nine cardinal positions of gaze.

The patient was then referred to the Ear, Nose, and Throat Department after ophthalmic examination because of the suspicion of acute sinusitis. Nasal endoscopy revealed acute bacterial rhinosinusitis, but no nasal polyp, mass, or orbital complication from sinusitis was detected. The patient underwent blood tests, with normal complete blood count and mild elevations of erythrocyte sedimentation rate and high-sensitivity C-reactive protein. He also showed negativity for serum acetylcholine receptor antibodies. Magnetic resonance imaging (MRI) examination of the brain and orbit with contrast was urgently requested to rule out space-occupying lesions and other potential

intracranial abnormalities. The MRI revealed no mass, aneurysm, infarction, or hemorrhage; however, it did depict fluid opacification in the left frontal, bilateral ethmoid, and left maxillary sinuses, with no bony erosion. Thin enhancing dura along the left inferior frontal region, adjacent to the left frontal sinus, and mild abnormal enhancing soft-tissue thickening at the superior extraconal space of the left orbit were also noted. There was no evidence of inflammation or injury of bilateral extraocular muscles, including the levator palpebrae superioris (LPS) muscle, and no orbital inflammation or fat stranding were identified (Figure 3).

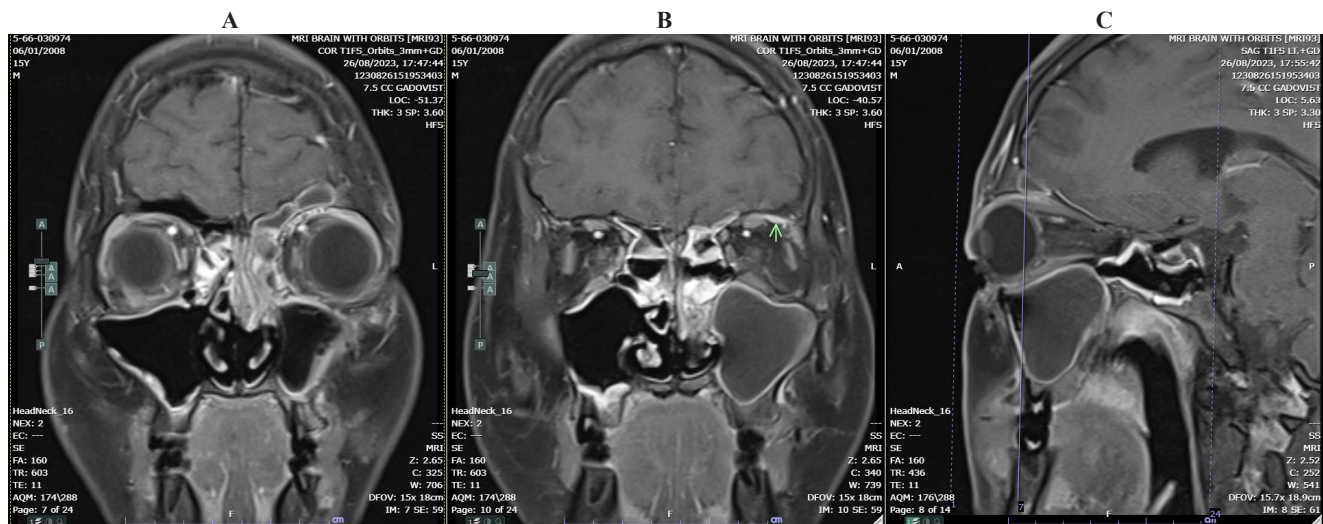


Figure 3 Magnetic resonance imaging (T1 with contrast). (A, B) Coronal views demonstrated left-sided fronto-ethmoidal sinusitis with abnormal contrast enhancing dura along the inferior frontal region and superior extraconal space of the left orbit (arrow). (C) A sagittal view revealed left-sided frontal sinus mucosal thickening with enhancing inflammation.

An otolaryngologist prescribed a once-daily high intravenous dose of levofloxacin (750 mg). The patient achieved complete recovery from the left-sided upper-eyelid ptosis after 5 days of this treatment. In addition, the frontal headache and nasal discharge were ameliorated. The patient was discharged from hospital 7 days after admission.

Discussion

Acquired isolated oculomotor nerve palsy or CN III palsy is typically caused by an aneurysm, brain ischemia, a neoplasm, head trauma, or diabetes mellitus.⁵ In addition, Ng et al. proposed that pediatric CN III palsy results most commonly from congenital, traumatic, and tumor-related causes.² The proximity

of the facial sinuses and the orbit can lead to orbital complications secondary to sinusitis. However, sinus diseases involving palsy of the superior division of CN III have rarely been reported. Most patients with such palsy have been diagnosed with sphenoid sinusitis.⁶⁻¹⁰ To the best of our knowledge, only three cases of palsy of the superior branch of CN III associated with frontal sinus disease have been reported.^{4,11,12} Moreover, only one patient has been described as having CN III palsy presenting with only isolated ptosis caused by frontal sinusitis.⁴

Anatomically, the oculomotor nerve or CN III divides into the superior and inferior rami near the anterior cavernous sinus or posterior orbit. Then, the superior ramus passes along the upper part of the lateral wall of the sphenoidal and posterior ethmoidal sinuses.¹³ The LPS and superior rectus muscle are supplied by the superior ramus, whereas the medial and inferior recti, inferior oblique, and ciliary ganglion are supplied by the inferior ramus. Clinically, upper-eyelid ptosis and limited supraduction of the eye characterize paresis of the superior division of CN III.

In two case reports, Ajinkya et al.⁹ and Yen Nee See et al.¹⁰ stated that isolated ptosis could be explained by partial compression of the superior ramus of CN III by adjacent structures, including inflamed sinuses. The distal branch of this nerve innervates the LPS and superior rectus muscle. Isolated ptosis with no abnormalities of the motility of extraocular muscles can be the result of a compromised LPS supplied by this distal branch. However, both of the above mentioned cases involved patients with sphenoid sinusitis. Meanwhile, Park et al. claimed to have encountered a case in which frontal sinus infection directly spread to the superior orbit through the defective inferior wall of the frontal sinus.¹² In contrast to their findings obtained by computed tomography, no orbital bone erosion or defects were found by MRI in the present case. In

addition, their patient presented not only with unilateral ptosis but also with ipsilateral limited supraduction. However, Mirza et al.⁴ postulated another mechanism by which isolated ptosis can occur. Specifically, they identified partially localized inflammation of the superior ramus of CN III due to COVID-19 infection. It is thus possible that, in the current case, the patient's influenza A infection could have had similar effects.

Although one report described palsy of the superior ramus of CN III presenting with isolated upper-eyelid ptosis with no ophthalmoplegia, pupillary involvement, or orbital signs from frontal sinusitis, the patient was an adult.⁴ With the dramatic resolution of the upper-eyelid ptosis after the initiation of intravenous antibiotics, the authors assumed that the frontal sinusitis found using MRI was the main cause in that case. In addition, the sphenoid sinus was not inflamed in this patient. Given the patient's afebrile status and normal total white blood cell count in the present case, it was supposed that the preceding influenza A infection had caused the frontal sinusitis. MRI was urgently scheduled and performed on this patient to rule out an intracranial cause of the acute ptosis combined with headache, such as intracranial bleeding, the rupture of a posterior communicating artery aneurysm, and mass compression. The MRI also immediately ruled out other concerns, including midbrain infarction and cavernous sinus thrombosis as a complication of sinusitis.

Owing to the absence of facial anhidrosis or pupil constriction, Horner's syndrome could also be ruled out. Another differential diagnosis was myasthenia gravis, but this patient lacked typical myasthenia gravis lid signs, fluctuating weakness, diplopia, and fatigability. Myositis affecting only the LPS was another possible differential diagnosis.^{14,15} However, MRI did not reveal any evidence of an inflamed or injured LPS, and the patient was negative for serum acetylcholine receptor antibodies. In addition, he confirmed a lack of any

history of treatment with botulinum toxin on the upper face.

This case should raise awareness of the possibility of sinusitis complications. This case also shows that preceding influenza A infection may contribute to the development of isolated ptosis.

When ptosis is accompanied by other neurological deficits such as ophthalmoplegia, pupillary miosis, or mydriasis suggestive of CN III palsy, Horner's syndrome, imaging of the brain, orbits, or cerebrovascular system should typically be performed on an urgent basis.¹⁶ Computed tomography plays an important role in ruling out serious intracranial abnormalities as a cause of ptosis and achieving a rapid diagnosis of sinusitis when cases have an atypical presentation. However, contrast-enhanced MRI is the imaging modality of choice and provides much more detailed findings of the orbit and its surroundings.

Conclusion

There has been little focus on sinusitis associated with palsy of the superior division of CN III. This report describes an uncommon presentation of a pediatric patient with palsy of the superior branch of CN III presenting with only isolated ptosis caused by frontal sinusitis. It highlights a potential complication of acute sinusitis and raises awareness of a rare differential diagnosis in isolated, unilateral ptosis. Diagnostic neuroimaging may help the management of such atypical cases.

Acknowledgments

We thank Tom Buckle from Scribendi (www.scribendi.com) for editing a draft of this manuscript.

Ethics Approval

This report was approved by the Institutional Review Board (IRB) of Police General Hospital,

Bangkok, Thailand (IRB number: Dh100-66). Informed consent was obtained from the patient and his parents to publish the details of this case. All confidential data were kept in a secured database.

Disclosure

The author declares no conflicts of interest in this work.

References

1. Latting MW, Huggins AB, Marx DP, Giacometti JN. Clinical evaluation of blepharoptosis: distinguishing age-related ptosis from masquerade conditions. *Semin Plast Surg.* 2017;31(1):5-16.
2. Ng, Y.S., Lyons, Oculomotor nerve palsy in childhood. *Canadian journal of Ophthalmology/Journal Canadien d'Ophthalmologie,* 2005;40(5):645-53.
3. Lawson W, Reino AJ. Isolated sphenoid sinus disease: an analysis of 132 cases. *Laryngoscope.* 1997.107(12): 1590-5.
4. Mirza MO, Mathai A, Owens A, et al. Acute unilateral isolated ptosis as a complication of sinusitis in a post-COVID-19 patient. *BMJ Case Rep.* 2023 May 2;16(5).
5. Richards BW, Jones FR Jr, Younge BR. Causes and prognosis in 4,278 cases of paralysis of the oculomotor, trochlear, and abducens cranial nerves. *Am J Ophthalmol* 1992;113:489-96.
6. Stefanis L, Przedborski S. Isolated palsy of the superior branch of the oculomotor nerve due to chronic erosive sphenoid sinusitis. *J Clin Neuroophthalmol* 1993; 13:229-31.
7. Celebisoy N, Celebisoy M, Tokucoglu F, et al. Superior division paresis of the oculomotor nerve: report of four cases. *Eur Neurol* 2006; 56:50-3.
8. Chotmongkol V, Chainunsamit S. Superior branch palsy of the oculomotor nerve caused by acute sphenoid sinusitis. *J Med Assoc Thai* 1999; 82:410-3.
9. Ajinkya A, Kelkar, Sarang Pabalkar. Isolated Unilateral Ptosis Presenting as a Complication of Acute Rhinosinusitis: Case Report. *Open Journal of Otolaryngology*2020;3(2): p.5-8.

10. Wendy Yen Nee See, Kala Sumugam, Visvaraja Subrayan. Unilateral ptosis as the sole presenting symptom in a case of partial third nerve palsy and bilateral sphenoid sinusitis in a child. *EyeSEA* 2018; 13(1):68-72.
11. Lin CJ, Kao CH, Kang BH, et al. Frontal sinus mucocele presenting as oculomotor nerve palsy. *Otorhinolaryngol Head Neck Surg* 2002;126:588-90.
12. Park DY, Baek BJ. Superior Branch Palsy of the Oculomotor Nerve Caused by Frontal Sinusitis. *J Craniofac Surg*. 2016 May;27(3):e248-9.
13. El Mograbi A, Soudry E. Ocular cranial nerve palsies secondary to sphenoid sinusitis. *World J Otorhinolaryngol Head Neck Surg* 2017;3:49-53.
14. Court JH, Janicek D. Acute unilateral isolated ptosis. *BMJ Case Rep* 2015;2015:bcr2014207720.
15. Abdrabou AM. Levator palpebrae superioris myositis as an unusual cause of unilateral ptosis-case report. *Egypt J Radiol Nucl Med* 2021;52.
16. Keene KR, Kan HE, van der Meeren S, et al. Clinical and imaging clues to the diagnosis and follow-up of ptosis and ophthalmoparesis. *J Cachexia Sarcopenia Muscle* 2022 Dec;13(6):2820-34.

รายงานผู้ป่วย : ภาวะเปลือกตาตกที่เกิดจากโรคไชนัสอักเสบ



Busayanut Puangsricharoen, MD

บุษยณัฐ พวงศรีเจริญ, พ.บ.

บทคัดย่อ:

วัตถุประสงค์: ภาวะเปลือกตาตกเกิดจากหลายสาเหตุ ได้แก่ เปลือกตาตกหลังอุบัติเหตุ (traumatic) จากการถูกดึงถ่วง (mechanical) จากระบบประสาท (neurogenic) จากภาวะกล้ามเนื้อเปลือกตาอ่อนแรง (myogenic) อย่างไรก็ตามภาวะเปลือกตาตกที่เกิดจากประสาทสมองเส้นที่ 3 อัมพาตร่วมกับไทรอยด์ที่บริเวณหน้าผากอักเสบพบได้น้อยมาก ผู้วิจัยรายงานผู้ป่วยเด็กชายอายุ 15 ปี ที่มีเปลือกตาข้างซ้ายตกจากประสาทสมองเส้นที่ 3 อัมพาต ร่วมกับไทรอยด์ที่บริเวณหน้าผากอักเสบ

รายงานผู้ป่วย: เด็กชายไทยอายุ 15 ปี มาด้วยเปลือกตาข้างซ้ายตก 2 วัน โดยมีการติดเชื้อไวรัสไข้หวัดใหญ่สายพันธุ์เอนำมา ก่อน 1 สัปดาห์ การตรวจการเคลื่อนไหวของลูกตาและรูม่านตาปกติ ผลการตรวจด้วยคลื่นแม่เหล็กไฟฟ้าบริเวณสมองและใบหน้าพบไทรอยด์อักเสบและเนื้อเยื่อรอบๆ บวมโดยเฉพาะไทรอยด์หน้าผากด้านซ้าย โดยไม่พบความผิดปกติที่กล้ามเนื้อลิฟตา (levator palabrae superior) ผู้ป่วยได้รับการวินิจฉัยว่าเป็นประสาทสมองเส้นที่ 3 อัมพาต ร่วมกับไทรอยด์ที่บริเวณหน้าผากอักเสบ ภาวะเปลือกตาตกหายหลังผู้ป่วยได้รับยาปฏิชีวนะลิโวฟลอกซาซินทางเส้นเลือดเป็นเวลา 5 วัน

สรุป: ไทรอยด์ที่บริเวณหน้าผากอักเสบก่อให้เกิดประสาทสมองเส้นที่ 3 อัมพาตได้ ซึ่งอาจมาด้วยภาวะเปลือกตาตกอย่างเดียว กรณีศึกษานี้ชี้ให้เห็นถึงผลแทรกซ้อนของไทรอยด์อักเสบและความสำคัญในการวินิจฉัยผู้ป่วยที่มาด้วยเปลือกตาตกข้างเดียว ซึ่งการตรวจด้วยคลื่นแม่เหล็กไฟฟ้าบริเวณสมองและใบหน้าสามารถช่วยในการวินิจฉัยในกรณีศึกษานี้

คำสำคัญ: ประสาทสมองเส้นที่ 3, อัมพาต, ประสาทกล้ามเนื้อตาอัมพาต, เด็ก, เปลือกตาตก, ไชนัสอักเสบ

กลุ่มงานตา โรงพยาบาลตำรวจ

Footnotes and Financial Disclosures

Originally receive: 24/9/2024

Final revision: 12/11/2025

Accepted: 13/11/2025

Corresponding author: **Busayanut Puangsricharoen**

Department of Ophthalmology, Police General Hospital, Bangkok, Thailand

Tel.: +662 207 6000

Fax: +662 252 8080

Email: busayanutp126@gmail.com

Adult Orbital Xanthogranuloma: A Case Report

Paphitchaya Temphattharachok, MD*

Monkol Uiprasertkul, MD†

Sunisa Sintuwong, MD, MPPM, MSc*

Abstract

Objectives: To report a rare case of adult orbital xanthogranuloma (AOX).

Methods: We describe a 39-year-old Thai woman with progressive bilateral eyelid swelling and for 5 years and yellowish discoloration of the left lower eyelid for 2 years.

Results: An earlier biopsy of the left lacrimal gland at another hospital showed dacryoadenitis. She received oral prednisolone with good initial response, but symptoms recurred after discontinuation. At presentation, she had bilateral eyelid swelling, yellowish discoloration of the left lower eyelid, bilateral lacrimal glands enlargement, and right eye proptosis, without infection. Orbital computed tomography (CT) demonstrated mildly enhancing infiltrative soft tissue in both periorbital regions and lacrimal glands, without bony destruction. A repeat biopsy of the yellowish lesion revealed foamy macrophages and small lymphoid cells. No systemic involvement was identified. Clinical and histopathological findings supported a diagnosis of AOX, the rarest subtype of adult orbital xanthogranulomatous disease (AOXGD AXDO). Oral corticosteroid therapy was initiated.

Conclusions: AOX is a rare orbital disorder that should be considered in the differential diagnosis of orbital disease. Systemic evaluation is essential due to potential associations in other subtypes. Although various treatment approaches have been reported, no standard therapy exists. Further studies are required to clarify disease mechanisms and management.

Keywords: Adult orbital xanthogranuloma, xanthogranulomatous disease, orbit, eyelid swelling, non-Langerhans cell histiocytosis, corticosteroid therapy

*Department of Ophthalmology, Mettaphrarak (Wat Rai Khing) Hospital, Nakhon Pathom, Thailand

†Department of Pathology, Siriraj Hospital, Mahidol University, Thailand

Introduction

Orbital xanthogranulomatous disease belongs to class II non-Langerhans cell histiocytoses and represents a distinctly uncommon clinical condition¹⁻⁶. It encompasses a heterogeneous spectrum of rare disorders that share characteristic cutaneous manifestations and histopathological profiles. Four clinical subtypes are recognized: adult-onset xanthogranuloma (AOX), adult-onset asthma and periocular xanthogranuloma (AAPOX), necrobiotic xanthogranuloma (NBX), and Erdheim–Chester disease (ECD). Systemic manifestations and multi-organ involvement may occur in some subtypes.

The true prevalence of orbital xanthogranulomatous disease remains unknown, as no population-based epidemiological studies have been published. Available data are limited to case reports and small series. Among the subtypes, NBX appears to be the most frequently reported, followed by ECD and AAPOX, whereas AOX is considered the least common form³⁻⁶.

We report a case of AOX, the least common subtype.

Case Report

A 39-year-old woman with a history of thyrotoxicosis (currently euthyroid) presented with progressive, painless bilateral upper eyelid swelling for 5 years without lower eyelid involvement. Three years earlier, she had been evaluated at a government hospital in Bangkok, where she underwent an incisional biopsy. The pathological result was dacryoadenitis. She was prescribed oral steroids, with good response, but discontinued treatment on her own after 2 months and was lost to follow-up. Her bilateral upper eyelids swelling recurred within a few months. Six months prior to presentation at our hospital, she developed bilateral lower eyelid swelling and yellowish discoloration of the left lower eyelid, accompanied by periocular discomfort (Figure 1A).

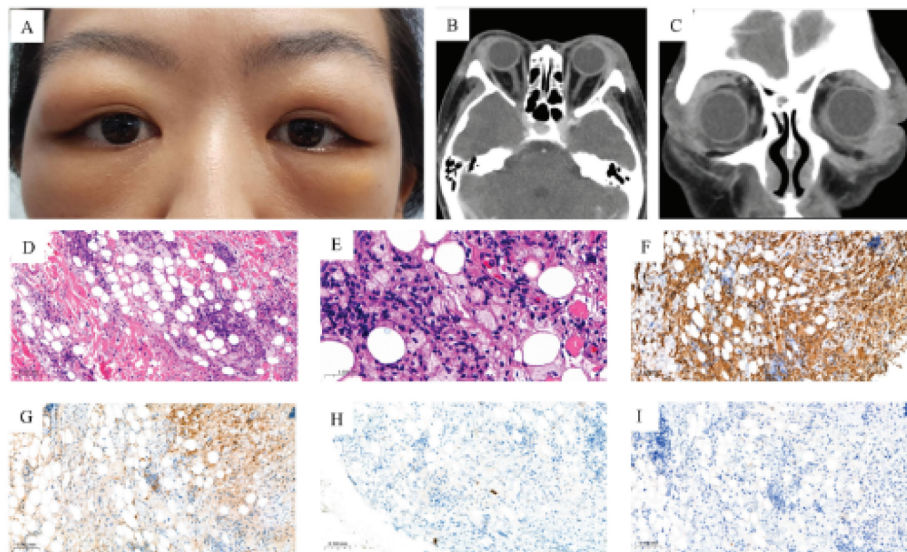


Figure 1 A 39-year-old Thai woman presented progressive painless bilateral upper and lower eyelids swelling for 5 years and yellow skin discoloration at left lower eyelid for 2 years. Bilateral lacrimal gland enlargements and proptosis of her right eye were detected. There were no other signs and symptoms of infection (A). CT scan of the orbit showed mild enhancing infiltrative soft tissue in both periorbital areas and lacrimal glands without bony destruction (B, C). An incisional biopsy was conducted at the area of yellow skin discoloration, which revealed the presence of foamy macrophages and small lymphoid cells in H & E (D, E), Positive for CD 68 (F), factor XIIIa (G) and negative for CD1a (H) and SI00 (I). No systemic involvement has been detected in this patient. Based on her clinical and histopathological feature, a diagnosis of adult orbital xanthogranulomatous disease, adult xanthogranulomatous disease of the orbit (AOX) subtype was made. Oral prednidolone 1 mg/kg/day was prescribed. The patient responded well to it.

Examination:

- Best corrected VA: 20/20 OU
- IOP: 16 mmHg OU
- Bilateral upper and lower eyelid swelling with a painless, well-circumscribed, firm mass in the superolateral region
- Yellow discoloration above the left lower eyelid mass
- Extraocular movements: full in all directions
- Hertel exophthalmometry: 14 mm OD, 12 mm OS
- No palpable lymphadenopathy
- Cardiopulmonary and systemic examinations: within normal limits

Investigations:

- Contrast-enhanced orbital computed tomography (CT) (Figure 1B and 1C): mild bilateral proptosis; mildly enhancing infiltrative soft tissue involving both periorbital regions and lacrimal glands;

no bony destruction; and extraocular muscles and orbital fat are unremarkable.

- Histopathology: aggregates of foamy macrophages and small lymphoid cells (Figure 1D and 1E).

- Immunohistochemistry: positive for factor CD68 (Figure 1F), XIIIa (Figure 1G); negative for CD1a (Figure 1H) and S-100 (Figure 1I).

- Systemic evaluation: normal complete blood count (CBC), echocardiogram, chest-abdomen computed tomography, and long-bone radiographs.

A diagnosis of AOX was made. Oral corticosteroid therapy (1 mg/kg/day) was initiated, with the dosage tapered by 10 mg every two weeks. She responded well to treatment; eyelid swelling decreased and discomfort resolved (Figure 2). We planned to maintain oral corticosteroids at 10 mg for at least six months. If clinical worsening occurs, immunosuppressive drugs will be considered.



Figure 2 The patient at the 3-month follow-up after oral prednisolone treatment.

Discussion

Within the group of non-Langerhans cell histiocytoses, orbital xanthogranulomatous disease is categorized as class II and is considered rare¹⁻⁶. No epidemiological study has provided population-based prevalence figures, and current knowledge is derived almost entirely from isolated case reports and small series. Among the four subtypes, NBX is most frequently reported, followed by ECD

and AAPOX, with AOX representing the least common presentation³⁻⁶. The initial description of adult-onset xanthogranuloma was reported in 1963 by Gartmann and Tritsch. Approximately 10% of juvenile xanthogranulomas are found in adults^{2,3}. Most cases occur in middle-aged patients, with no gender predilection, presenting as well-circumscribed, firm, yellow-orange lesions predominantly in the head and neck⁴.

AOX is the least common subtype and usually has a favorable prognosis without systemic disease. AAPOX is associated with asthma and may present with lymphadenopathy and elevated IgG levels¹. NBX is characterized by ulcerated, fibrosing cutaneous lesions and is frequently associated with paraproteinemia and multiple myeloma⁵. ECD represents the most aggressive subtype, involving progressive fibrosclerosis of orbital and systemic tissues, with a high mortality rate despite treatment⁵.

Despite clinical variability, all subtypes of AOXGD demonstrate overlapping histo-pathological features, notably aggregates of foamy histiocytes, lymphocytes, plasma cells, and Touton giant cells. Immunohistochemically, the foamy histiocytes are strongly positive for CD68, CD163, and factor XIIIa, but negative for CD1a and S-100⁵.

Our patient's clinical presentation—progressive eyelid and periorbital swelling with yellowish discoloration of the left lower eyelid and bilateral lacrimal gland enlargement, but no systemic involvement—was consistent with AOX. She responded well to oral corticosteroid therapy.

At present, there is no disease-specific targeted therapy available for AOX. Treatment approaches reported include corticosteroids (topical, intralesional, systemic), alkylating agents such as chlorambucil and melphalan, antimetabolites, interferon alpha-2b, radiotherapy, plasmapheresis, and carbon dioxide laser therapy. Prognosis for AOX remains more favorable compared with other subtypes.

Conclusion

Adult orbital xanthogranuloma (AOX) is an uncommon subtype of orbital xanthogranulomatous disease that can mimic other orbital inflammatory conditions. Our case highlights the importance of

considering AOX in the differential diagnosis of persistent eyelid and lacrimal gland swelling with characteristic yellowish discoloration. Histopathology remains essential for confirmation, and systemic evaluation is mandatory to exclude associated subtypes with multi-organ involvement. Although corticosteroids remain the mainstay of treatment, long-term management strategies have yet to be standardized. Greater awareness and further studies are required to improve understanding of disease behavior, guide treatment, and optimize outcomes for affected patients.

References

1. Jakobiec FA, Mills MD, Hidayat AA, Dallow RL, Townsend DJ, Brinker E, et al. Periocular xanthogranulomas associated with severe adult-onset asthma. *Trans Am Ophthalmol Soc.* 1993;91:99-125.
2. Achar A, Naskar B, Mondal PC, Pal M. Multiple generalized xanthogranuloma in adult: case report and treatment. *Indian J Dermatol.* 2011;56(2):197-200.
3. Bastianpillai J, Haloob N, Panchappa S, Marais J. The rare case of an adult-onset xanthogranuloma of the paranasal sinuses: a histological dilemma. *Case Rep Pathol.* 2020;2020:1-4. doi:10.1155/2020/8832802.
4. Wiffen J, Kalantary A, Ardakani NM, Turner A. Adult onset xanthogranuloma of the eyelid. *Am J Ophthalmol Case Rep.* 2023;29:101775. doi:10.1016/j.ajoc.2023.101775.
5. Kerstetter J, Wang J. Adult orbital xanthogranulomatous disease: a review with emphasis on etiology, systemic associations, diagnostic tools, and treatment. *Dermatol Clin.* 2015;33(3):457-63. doi:10.1016/j.det.2015.03.009.
6. Kumawat D, Nayak S, Goel R, Beniwal M, Rajesh R, Chawla R. Bilateral adult-onset orbital xanthogranuloma: a case report and review of literature. *Indian J Ophthalmol Case Rep.* 2023;3(1):113-6. doi:10.4103/ijocr.ijocr_122_22.

รายงานผู้ป่วย: ก้อนอักเสบเรื้อรังสีเหลืองบริเวณเบ้าตาในผู้ใหญ่ (Adult Orbital Xanthogranuloma)



Paphitchaya Temphattharachok, MD
ปพิชญา เต็มภัทรโชค, พ.บ.*



Monkol Uiprasertkul, MD
มงคล อุยประเสริฐกุล, พ.บ.†



Sunisa Sintuwong, MD, MPPM, MSc
สุนิสา สินธุวงศ์, พ.บ.*

บทคัดย่อ:

วัตถุประสงค์: รายงานกรณีศึกษาผู้ป่วยโรคก้อนอักเสบเรื้อรังสีเหลืองบริเวณเบ้าตาในผู้ใหญ่ (adult orbital xanthogranuloma; AOX) ซึ่งเป็นโรคที่พบน้อยมาก

วิธีการ: ผู้ป่วยหญิงไทยอายุ 39 ปี มีอาการบวมของเปลือกตาทั้งสองข้างอย่างค่อยเป็นค่อยไปนาน 5 ปี และมีรอยเหลืองบริเวณเปลือกตาล่างซ้ายมา 2 ปี

ผลการรักษา: ผลการตรวจชิ้นเนื้อของต่อน้ำตาจากโรงพยาบาลเดิมแสดงลักษณะของต่อน้ำตาอักเสบ (dacryoadenitis) ผู้ป่วยเคยได้รับยาสเตียรอยด์ชนิดรับประทานตอนต้นในระยะแรก แต่กลับมามีอาการซ้ำหลังหยุดยาเอง ครั้งนี้เมื่อมาพบแพทย์ตรวจร่างกายพบมีอาการบวมของเปลือกตาทั้งสองข้าง มีรอยสีเหลืองบริเวณเปลือกตาล่างซ้าย และต่อน้ำตาโต แต่ไม่มีสัญญาณการติดเชื้อ ภาพเอกซเรย์คอมพิวเตอร์ของเบ้าตาแสดงให้เห็นเนื้อเยื่ออ่อนอักเสบแทรกซึมในเนื้อเยื่อปกติ (mildly enhancing infiltrative soft tissue) บริเวณรอบเบ้าตาและต่อน้ำตาทั้งสองข้าง โดยไม่พบการทำลายกระดูก การตรวจชิ้นเนื้อซ้ำบริเวณรอยเหลืองพบ foamy macrophages และเซลล์น้ำเหลืองขนาดเล็ก ผลการตรวจระบบอื่นไม่พบความผิดปกติ จากการซักประวัติและตรวจร่างกาย ตลอดจนเครื่องมือพิเศษและการตรวจทางพยาธิวิทยา จึงให้การวินิจฉัยว่า เป็นโรคก้อนอักเสบเรื้อรังสีเหลืองบริเวณเบ้าตาในผู้ใหญ่ หรือ AOX ซึ่งเป็นชนิดที่พบน้อยที่สุดของกลุ่มโรคก้อนอักเสบเรื้อรังสีเหลืองบริเวณเบ้าตาในผู้ใหญ่ adult orbital xanthogranulomatous disease (AOXGD) และได้เริ่มให้การรักษาด้วยยาสเตียรอยด์ชนิดรับประทาน ในผู้ป่วยรายนี้

สรุป: โรคก้อนอักเสบเรื้อรังสีเหลืองบริเวณเบ้าตาในผู้ใหญ่ เป็นโรคในเบ้าตาที่พบน้อย ควรนึกถึงในการวินิจฉัยแยกโรคของภาวะอักเสบหรือบวมของเบ้าตา และการตรวจทางพยาธิวิทยามีความจำเป็นต่อการยืนยันผลการวินิจฉัย และการตรวจร่างกายให้ครบทุกระบบมีความจำเป็นในการแยกชนิดจำเพาะ (subtype) ของกลุ่มโรคนี้ แม้ว่าการรักษาด้วยยาสเตียรอยด์ได้ผลดีในคนไข้หลายคนที่ถูกวินิจฉัยด้วยโรคนี้ แต่ในปัจจุบันยังไม่มีแนวทางการรักษามาตรฐานและจำเพาะ ดังนั้นจำเป็นต้องมีการศึกษาต่อไปเพื่อทำความเข้าใจกลไกของโรคและแนวทางการจัดการที่เหมาะสมต่อไป

คำสำคัญ: ก้อนอักเสบเรื้อรังสีเหลืองบริเวณเบ้าตาในผู้ใหญ่, เบ้าตา, เปลือกตาบวม, กลุ่มของโรคที่เกิดจากการเพิ่มจำนวนมากผิดปกติของเซลล์เม็ดเลือดขาวชนิดอื่นที่ไม่ใช่เซลล์ลางเกอร์ฮานส์, ยาสเตียรอยด์

* แผนกจักษุวิทยา โรงพยาบาลเมตตาประชารักษ์ (วัดไร่ขิง) จังหวัดนครปฐม

† แผนกพยาธิวิทยา โรงพยาบาลศิริราช มหาวิทยาลัยมหิดล

Footnotes and Financial Disclosures

Originally receive: 30/9/2025

Final revision: 8/12/2025

Accepted: 10/12/2025

Financial disclosure:

The authors declare no financial or proprietary interest in any material or method mentioned.

Authorship statement:

All authors certify that they have made substantial contributions to the conception and design of the work, acquisition and interpretation of data, drafting and revising the article, gave final approval of the version to be published, and agree to be accountable for all aspects of the work.

Corresponding author: **Busayanut Puangsricharoen**

Sunisa Sintuwong, M.D., M.P.P.M., M.Sc.

Department of Ophthalmology, Mettapracharak (Wat Rai Khing) Hospital, Nakhon Pathom, Thailand

Tel: +6634388700 Email: drsunisa@gmail.com

Specific Ocular Findings Leading to the Diagnosis of Early-Onset Neurofibromatosis Type 2

Pittaya Phamonvaechavan, MD¹, Subongkoch Subhadhirasakul MD¹,
Rawi Jongpipatchai, MD¹, Supathida Jiamsawad, MD¹

Abstract

Background: Neurofibromatosis type 2 (NF2) genetic disorder primarily characterized by the central nervous system tumors, including intracranial schwannomas and meningiomas. Diagnosis is often delayed due to variable presentations, especially in pediatric patients where ophthalmologic abnormalities may be the earliest sign.

Case Presentation: A 4-year-old boy referred for ocular evaluation due to multiple café-au-lait macules. Initial examination revealed reduced visual acuity, bilateral iris mammillation, and left retinal hamartoma, raising suspicion of NF2. Despite glasses being prescribed, the patient was lost to follow-up and returned at age 8 with left eye visual deterioration. Subsequent examination identified a flame-like epiretinal membrane (ERM) in the right eye and a combined hamartoma of the retina and retinal pigment epithelium (CHRRPE) in the left eye. Magnetic Resonance Imaging (MRI) confirmed multiple cranial nerve schwannomas and a left optic nerve sheath meningioma (ONSM), confirming the NF2 diagnosis at age 10.

Discussion: Pediatric NF2 can present with distinctive ocular findings: cortical cataracts, ERMs, CHRRPE, and ONSMs, which may precede neurological symptoms. Early recognition of NF2 ocular signs is crucial for timely diagnosis and management, potentially reducing morbidity.

Conclusion: This case highlights importance of thorough ophthalmologic evaluation in NF2 children. Early diagnosis can guide appropriate multidisciplinary management, improving prognosis in pediatric NF2 patients.

Keywords: Retinal hamartoma, Pediatric ophthalmology, Optic nerve sheath meningioma, Neurofibromatosis Type 2, Neurofibromatosis, Pediatric neurofibromatosis

¹Department of Ophthalmology, Faculty of Medicine Siriraj Hospital,
Mahidol University, Bangkok 10700, Thailand

Background

Neurofibromatosis type 2 (NF2) is a rare inherited disorder characterized by central nervous system tumors, predominantly intracranial schwannomas and meningiomas.¹ First described by Wishart in 1822 as a case of skull, dura mater, and brain tumors causing deafness¹, NF2 has an estimated incidence ranging from 1 in 25,000 to 1 in 87,410 live births²⁻⁴. Bilateral vestibular schwannomas are the hallmark of NF2, but patients are also prone to develop other tumors, including multiple meningiomas, gliomas, and neurofibromas⁵⁻⁷. Ocular lesions, neuropathies, skin surface tumors, and glial hamartia are additional characteristic manifestations⁵⁻⁷. Genetic studies have linked NF2 to mutations of the NF2 gene on chromosome 22q12, resulting in multiple tumor development in nerve sheaths, with over half of cases representing de novo mutations⁵⁻⁷.

NF2 clinical courses are variable, ranging from early-onset multiple tumors to lifelong asymptomatic presentations^{8,9}. Diagnosis primarily relies on magnetic resonance imaging (MRI), potentially supported by genetic confirmation of NF2 gene mutations. The 2018 revised Neurofibromatosis Type 2 Diagnostic Criteria, based on the Manchester criteria for NF2, aid in diagnosis¹⁰. However, definitive diagnosis can be delayed due to the rarity of NF2 and its diverse clinical manifestations. Older adolescents and adults typically present with vestibular schwannomas, while

ophthalmologic abnormalities are common in children and young adolescents¹¹. This case report illustrates the characteristic ocular features that may present at a young age without neurologic or auditory symptoms, resulting in a 6-year diagnostic delay in this instance.

Case Presentation

A 4-year-old boy, referred by a pediatrician for ocular evaluation due to multiple café-au-lait macules on all extremities, presented with visual acuity of 20/100 in the right eye and 20/60 in the left (picture chart). Anterior segment examination revealed bilateral iris mamillation and a left focal cortical cataract. Fundus photography showed normal optic discs bilaterally, a right epiretinal membrane (ERM), and a left retinal astrocytic hamartoma (Figure 1A). Glasses were prescribed according to cycloplegic refraction (right eye, -1.00 -0.50 X 20; left eye, -1.50 -2.50 X 145), after which the patient was lost to follow-up.

During this period, the patient underwent bilateral lateral rectus recession for exotropia at a private hospital at age 6. At age 8, he returned to the eye clinic due to gradual vision loss in the left eye. Examination revealed finger-counting visual acuity in the left eye, a focal cortical cataract, and a relative afferent pupillary defect in the left eye. Fundus photography showed a pale disc and retinal hamartoma in the left eye, with an ERM in the right eye (Figure 1B).

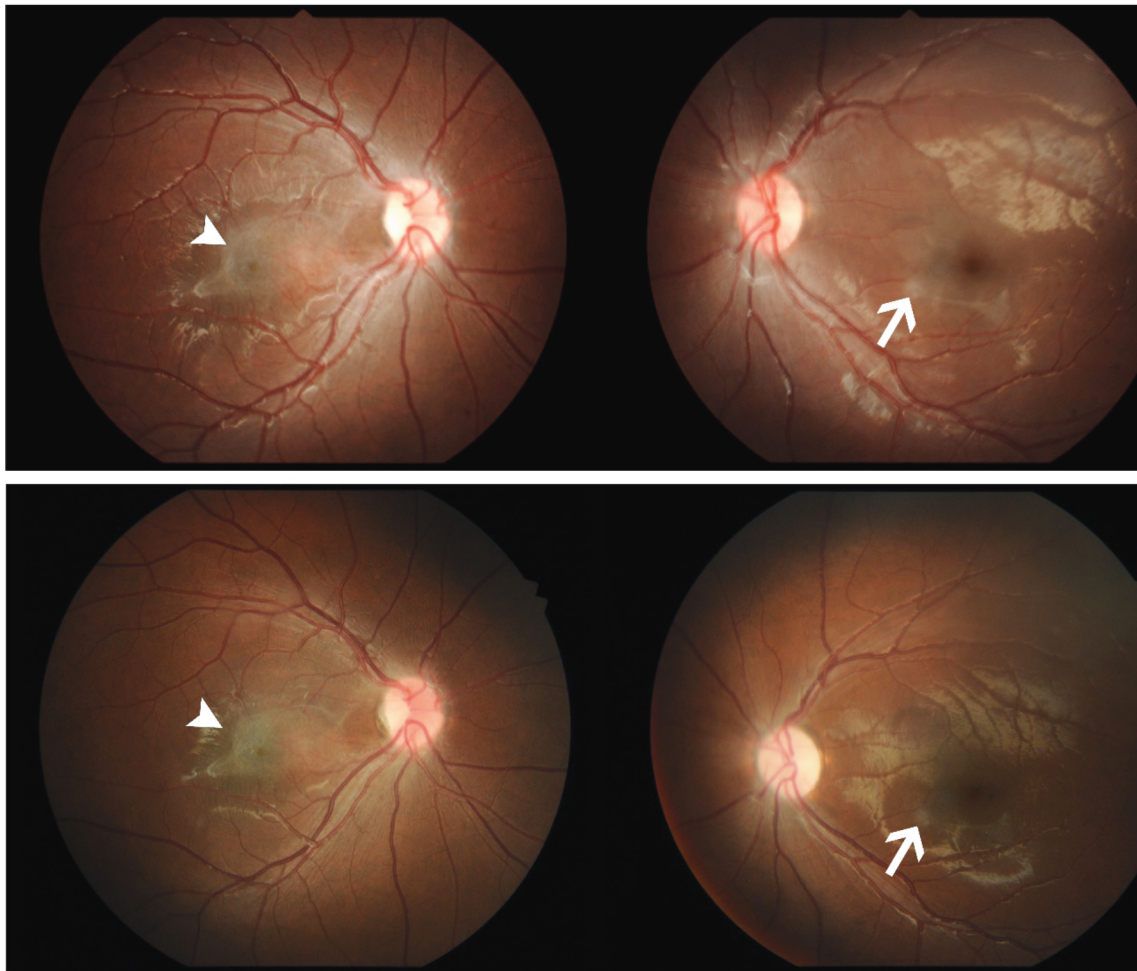


Figure 1 (A) Initial fundus photography of a 4-year-old boy showing an epiretinal membrane (arrowhead) in the right eye and a retinal hamartoma (arrow) in the left eye. (B) Fundus photography at age 10 years depicting an epiretinal membrane (arrowhead) in the right eye, along with a pale optic disc and a retinal hamartoma (arrow) in the left eye.

Investigations

Spectral-domain optical coherence tomography revealed a unique, flame-like ERM pattern in the vitreous of the right eye and a combined hamartoma of the retina and retinal pigment epithelium (CHRRPE) in the left eye (Figure 2). As NF2 was suspected, the boy was referred to the hospital's genetic clinic for further evaluation. He reported no hearing or neurological problems, and there was no family history of neurofibromatosis. Although his mother had nonspecific café-au-lait macules, she lacked other neurofibromatosis-associated symptoms.

MRI of the brain and orbits revealed multiple enhancing masses in bilateral cranial nerves (CN) V, right CN VI, bilateral CN VII, bilateral CN VIII, bilateral CN IX, bilateral CN X, and bilateral CN XI, suggestive of multiple schwannomas. A left optic nerve sheath meningioma (ONSM), a meningioma to the right of the cervicomedullary junction, and pressure on the optic nerve and left extraocular muscles (especially the left inferior rectus) were also detected. This pressure caused atrophic changes in the left optic nerve with optic neuropathy.

Based on these clinical and investigational

findings, the patient met the NF2 diagnostic criteria¹⁰, and a definitive diagnosis of NF2 was established at age 10. A multidisciplinary clinical evaluation

(otolaryngologist, pediatric neurologist, and neurosurgeon) was initiated. An audiogram and other hearing tests were unremarkable.

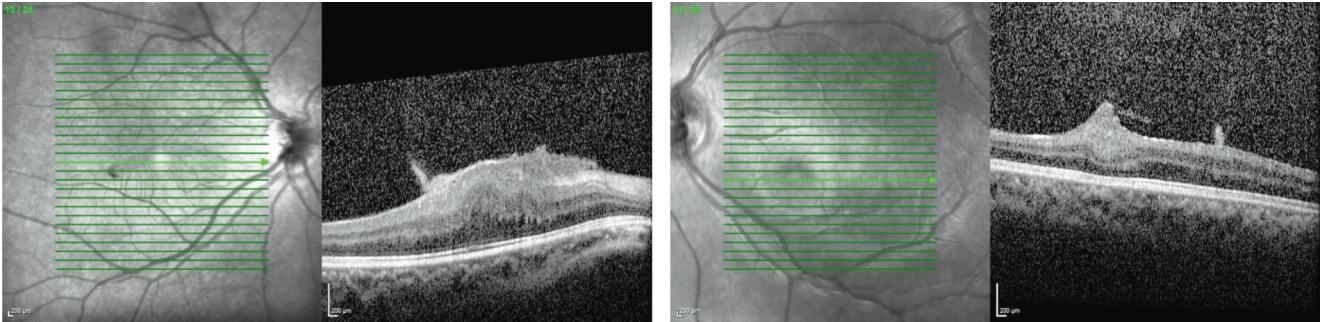


Figure 2 Spectral-domain optical coherence tomography illustrates the distinctive flame-like pattern of an epiretinal membrane extending into the vitreous in the right eye, and a combined hamartoma involving the retina and retinal pigment epithelium in the left eye.

Outcomes And Follow-Up

Due to the pressure effect of the meningioma involving the left optic nerve sheath, tumor removal was recommended to preserve left-eye vision. However, the patient's parents opted for close monitoring of the boy's symptoms instead.

Six months later, brain and whole-spine MRI (Figure 3) revealed increases in the sizes of the bilateral vestibular schwannomas, bilateral Meckel's cave schwannomas, right jugular foramen schwannomas, the cisternal part of right CN XII schwannomas, the left optic nerve meningioma, and the meningioma to

the right of the cervicomedullary junction extending to the C2 level. Left eye proptosis was also noted. Subsequently, the boy underwent left frontotemporal craniectomy with gross total resection of the orbital and tuberculum meningiomas to protect left eye vision. There were no immediate postoperative complications. One-month postoperative MRI showed no obvious residual tumor and a 50% improvement in proptosis. Additionally, radiation therapy was administered for the vestibular schwannomas. Tumor removal at the foramen magnum is planned upon completion of radiotherapy.

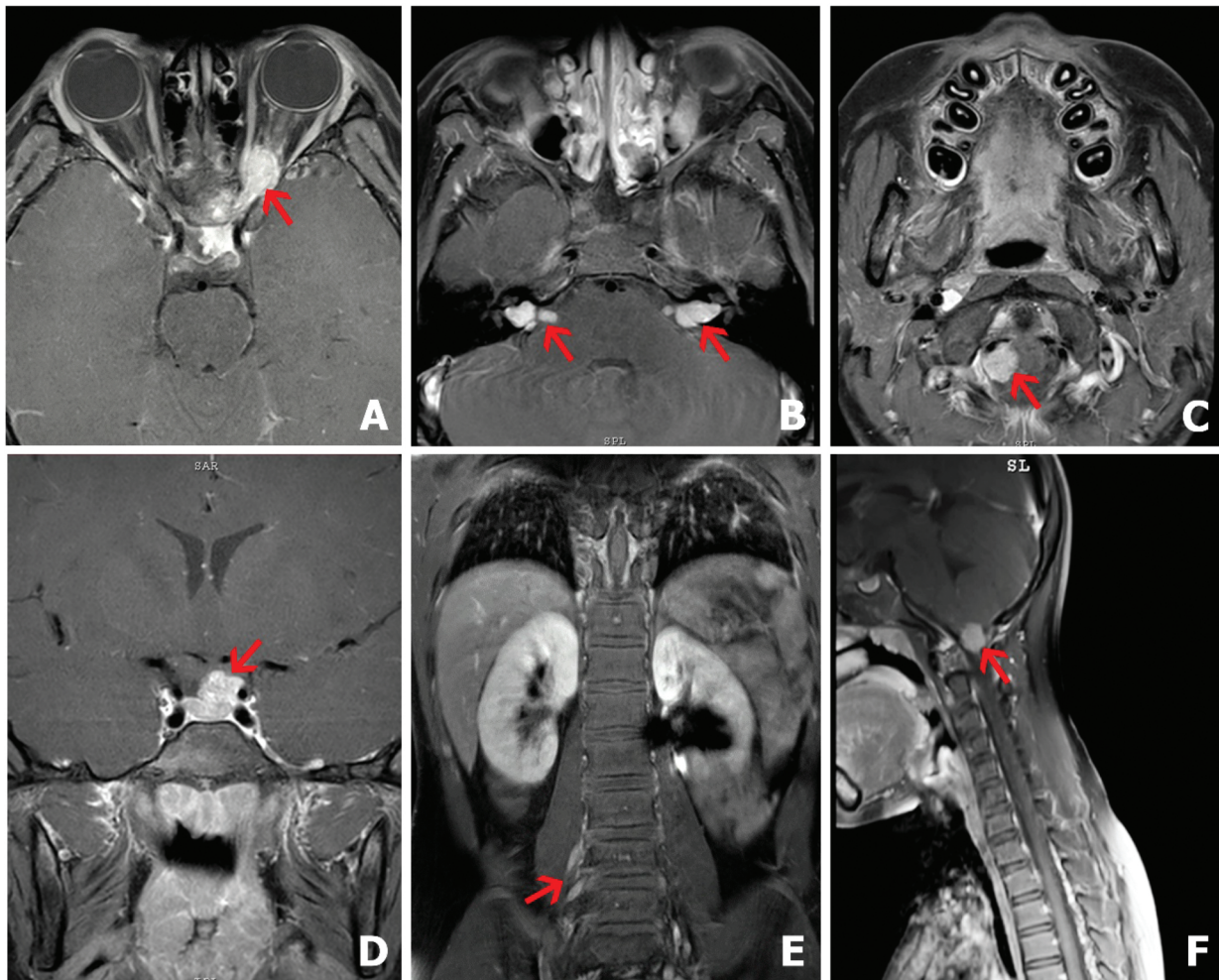


Figure 3 MRI T1-weighted images postgadolinium in axial and coronal planes demonstrate multiple tumors. (A) Left optic nerve sheath meningioma; (B) bilateral vestibular schwannomas (arrows); (C) right-sided meningioma at the cervicomedullary junction in axial and (F) sagittal views; (D) schwannoma on the left planum sphenoidale, partially extending to the pituitary fossa; and (E) meningiomas at the L4 and L5 nerve roots (arrows).

Discussion

NF2 is a rare, autosomal dominant disorder characterized by tumor predisposition. Early- and adult-onset NF2 exhibit distinct clinical presentations. Adult-onset NF2 typically manifests as hearing loss, tinnitus, or positional imbalance, indicative of CN VIII dysfunction¹²⁻¹⁴. Conversely, pediatric NF2 patients often present with nonvestibular nerve schwannomas (such as spinal cord tumors), extravestibular CN involvement, or ophthalmological symptoms¹²⁻¹⁴.

Gugel et al. reported a median age of diagnosis of 11 years (range 1–17 years) for nonfamilial NF2, with ophthalmological manifestations being the most common presenting symptom (49%)¹¹.

The patient described in this case report, a 4-year-old male with no family history of neurofibromatosis, initially presented with multiple café-au-lait macules on his extremities. Progressive blurry vision, predominantly in the left eye, developed subsequently. Ophthalmological examination revealed a cortical

cataract, a vertical flame-like ERM, CHRRPE, an astrocytic hamartoma, and an ONSM—all indicative of NF2¹²⁻¹⁴. Despite the absence of auditory symptoms, these NF2-specific ocular findings enabled an early diagnosis.

Several ocular findings of NF2 have been described in the literature, such as posterior subcapsular cataracts, wedge-shaped cortical cataracts, ERMs, and CHRRPE^{13,15}. In adults, ERMs may be associated with various retinal diseases and may not be a primary indicator of NF2. However, in children, ERMs are an important diagnostic finding for NF2. Several studies have reported a characteristic pattern of unusual, flame-like ERMs extending to the vitreous in spectral-domain optical coherence tomography findings¹⁶⁻¹⁸. This pattern is consistent with the ocular manifestations observed in the present case. Importantly, recognition of ERMs in children may facilitate early diagnosis of NF2, even in neurologically asymptomatic individuals with a severe phenotype of NF2¹⁹.

Furthermore, the present case shares similarities with a previously reported case of a 9-year-old boy who presented with CHRRPE, multiple presumed retinal astrocytic proliferations, and retinal astrocytic hamartomas²⁰. These hamartomas, considered a type of glial tumor of the retinal nerve fiber layer, are typically associated with tuberous sclerosis²¹. However, retinal astrocytic hamartomas can also be incidental findings on retinal examination and are rarely reported in neurofibromatosis patients.

Several studies have established a relationship between retinal hamartomas, CHRRPE, and NF2. In some instances, retinal hamartomas have been reported as a leading sign preceding the development of vestibular schwannomas²². Similarly, a meta-analysis revealed that retinal hamartomas were observed before the clinical diagnosis of NF2 in 11 out of 25 cases²³. These findings suggest that retinal hamartomas may be

a clue for diagnosing NF2. Recently, ERMs in children have been proposed as a diagnostic criterion for NF2¹⁹.

The progressive visual impairment in our reported case was caused by an ONSM compressing the left optic nerve. ONSMs are rare in pediatric patients, with an estimated prevalence of 1:95 000 to 1:525 000²⁴. Vision loss, optic atrophy, and optociliary shunt vessels constitute the classic clinical triad of ONSMs. In the present case, the ONSM was located in the intraconal part of the left orbit, directly compressing the left optic nerve.

Evidence supporting the association between NF2 and ONSM is growing. Bosch et al. reported a strong association between ONSMs and NF2 in a case series of NF2 patients.²⁵ Their findings also suggest that there is an increasing awareness of the potential presence of NF2 in patients diagnosed with ONSM.

Strabismus, reported in 52% of NF2 patients, can manifest as either comitant strabismus (exotropia, esotropia, or mixed horizontal and vertical deviation) or as cranial nerve palsies affecting CN III, CN IV, or CN VI²⁶. Our patient was diagnosed with exotropia and underwent bilateral lateral rectus recession. Strabismus has been documented in NF2 patients and may be the initial manifestation of NF2¹¹.

Children of NF2-affected parents are typically managed by NF2 specialists and undergo routine clinical screening and genetic testing, which facilitates timely diagnosis. In contrast, children without a family history of NF2 often face delayed diagnoses due to a lack of clinical awareness of initial symptoms. Children without vestibular schwannoma presentations have a mean diagnostic delay that is more than 12 months longer than that for children with a familial history of neurofibromatosis^{3,12}. Presentations involving nonvestibular tumors in childhood may suggest more aggressive forms of neurofibromatosis^{14,27}. Diagnosing NF2 at a young age can be particularly

challenging, leading to frequent diagnostic delays²⁸. Younger patients often exhibit more ophthalmologic signs and symptoms than older patients. Thorough ophthalmologic examinations are crucial for diagnosing rare inherited diseases such as NF2. Early recognition of NF2-specific ocular findings may enhance awareness and facilitate prompt diagnosis in pediatric patients.

In summary, the ophthalmic findings of NF2 can be subtle, necessitating a dilated fundus examination to detect peripheral cortical cataracts, ERMs, and retinal hamartomas. Our case exhibited all NF2-specific ocular findings: cortical cataracts, ERMs, retinal hamartomas, and ONSMs. Such findings are critical for diagnosing NF2, particularly in early-onset cases. Spectral-domain optical coherence tomography can reveal the distinctive flame-like pattern of ERMs. Early diagnosis and appropriate management can reduce morbidity in NF2 patients and significantly enhance their survival rate.

Learning Points/Take Home Messages

- Neurofibromatosis type 2-specific ocular findings are crucial for diagnosing the condition in early-onset cases.
- In young children, optical coherence tomography effectively demonstrates the unique flame-like pattern of epiretinal membranes.
- Early diagnosis, optimal management, and a multidisciplinary team approach are essential for reducing morbidity and improving the survival of patients with neurofibromatosis type 2.

References

1. Wishart JH. Case of Tumours in the Skull, Dura Mater, and Brain. *Edinb Med Surg J*. Jul 1 1822;18(72):393-397.
2. Antinheimo J, Sankila R, Carpen O, et al. Population-based analysis of sporadic and type 2 neurofibromatosis-associated meningiomas and schwannomas. *Neurology*. Jan 11 2000;54(1):71-6. doi:10.1212/wnl.54.1.71
3. Evans DG, Howard E, Giblin C, et al. Birth incidence and prevalence of tumor-prone syndromes: estimates from a UK family genetic register service. *Am J Med Genet A*. Feb 2010;152A(2):327-32. doi:10.1002/ajmg.a.33139
4. Evans DG, Moran A, King A, et al. Incidence of vestibular schwannoma and neurofibromatosis 2 in the North West of England over a 10-year period: higher incidence than previously thought. *Otol Neurotol*. Jan 2005;26(1):93-7. doi:10.1097/00129492-200501000-00016
5. Evans DG. Neurofibromatosis type 2 (NF2): a clinical and molecular review. *Orphanet J Rare Dis*. Jun 19 2009;4:16. doi:10.1186/1750-1172-4-16
6. Evans DG, Huson SM, Donnai D, et al. A clinical study of type 2 neurofibromatosis. *Q J Med*. Aug 1992;84(304):603-18.
7. Halliday D, Emmanouil B, Pretorius P, et al. Genetic Severity Score predicts clinical phenotype in NF2. *J Med Genet*. Oct 2017;54(10):657-664. doi:10.1136/jmedgenet-2017-104519
8. Coy S, Rashid R, Stemmer-Rachamimov A, et al. Correction to: An update on the CNS manifestations of neurofibromatosis type 2. *Acta Neuropathol*. Apr 2020;139(4):667. doi:10.1007/s00401-019-02044-6
9. Coy S, Rashid R, Stemmer-Rachamimov A, et al. An update on the CNS manifestations of neurofibromatosis type 2. *Acta Neuropathol*. Apr 2020;139(4):643-665. doi:10.1007/s00401-019-02029-5
10. Evans DG, King AT, Bowers NL, et al. Identifying the deficiencies of current diagnostic criteria for neurofibromatosis 2 using databases of 2777 individuals with molecular testing. *Genet Med*. Jul 2019;21(7):1525-1533. doi:10.1038/s41436-018-0384-y
11. Gugel I, Grimm F, Teuber C, et al. Presenting symptoms in children with neurofibromatosis type 2. *Childs Nerv Syst*. Oct 2020;36(10):2463-2470. doi:10.1007/s00381-020-04729-w
12. Anand G, Vasallo G, Spanou M, et al. Diagnosis of sporadic neurofibromatosis type 2 in the paediatric population. *Arch Dis Child*. May 2018;103(5):463-469. doi:10.1136/archdischild-2017-313154
13. Matsuo M, Ohno K, Ohtsuka F. Characterization of early onset neurofibromatosis type 2. *Brain Dev*.

- Feb 2014;36(2):148-52. doi:10.1016/j.braindev.2013.01.007
14. Ruggieri M, Iannetti P, Polizzi A, et al. Earliest clinical manifestations and natural history of neurofibromatosis type 2 (NF2) in childhood: a study of 24 patients. *Neuropediatrics*. Feb 2005;36(1):21-34. doi:10.1055/s-2005-837581
 15. McLaughlin ME, Pepin SM, Maccollin M, et al. Ocular pathologic findings of neurofibromatosis type 2. *Arch Ophthalmol*. Mar 2007;125(3):389-94. doi:10.1001/archophth.125.3.389
 16. Chan CC, Koch CA, Kaiser-Kupfer MI, et al. Loss of heterozygosity for the NF2 gene in retinal and optic nerve lesions of patients with neurofibromatosis 2. *J Pathol*. Sep 2002;198(1):14-20. doi:10.1002/path.1174
 17. Kang HM, Koh HJ, Chung EJ. Spectral-domain optical coherence tomography of combined hamartoma of the retina and retinal pigment epithelium in neurofibromatosis. *Korean J Ophthalmol*. Feb 2013;27(1):68-71. doi:10.3341/kjo.2013.27.1.68
 18. Waisberg V, Rodrigues LO, Nehemy MB, et al. Spectral-Domain Optical Coherence Tomography Findings in Neurofibromatosis Type 2. *Invest Ophthalmol Vis Sci*. Jul 1 2016;57(9):OCT262-7. doi:10.1167/iovs.15-18919
 19. Sisk RA, Berrocal AM, Scheffler AC, et al. Epiretinal membranes indicate a severe phenotype of neurofibromatosis type 2. *Retina*. Apr 2010;30(4 Suppl):S51-8. doi:10.1097/IAE.0b013e3181dc58bf
 20. Rishi P, Hirawat RS, Verma A. Association of bilateral, multiple presumed retinal astrocytic proliferations with combined hamartoma of retina and retinal pigment epithelium in a 9-year-old male child with neurofibromatosis type 2. *Indian J Ophthalmol*. Nov 2016;64(11):850-852. doi:10.4103/0301-4738.195609
 21. Martin K, Rossi V, Ferrucci S, et al. Retinal astrocytic hamartoma. *Optometry*. May 2010;81(5):221-33. doi:10.1016/j.optm.2009.12.009
 22. Chin EK, Almeida DR, Boldt HC. Combined Hamartoma of the Retina and Retinal Pigment Epithelium Leading to the Diagnosis of Neurofibromatosis Type 2. *JAMA Ophthalmol*. Sep 2015;133(9):e151289. doi:10.1001/jamaophthalmol.2015.1289
 23. Starosta DA, Lorenz B. [Retinal Astrocytic Hamartoma in Neurofibromatosis Type 2 - Metaanalysis and a Case Report]. *Klin Monbl Augenheilkd*. Mar 2018;235(3):290-300. Retinale astrozytäre Hamartome bei Neurofibromatose Typ 2 – Metaanalyse und Fallbericht. doi:10.1055/a-0583-0291
 24. Levin LA, Jakobiec FA. Optic nerve tumors of childhood: a decision-analytical approach to their diagnosis. *Int Ophthalmol Clin*. Winter 1992;32(1):223-40. doi:10.1097/00004397-199203210-00017
 25. Bosch MM, Wichmann WW, Boltshauser E, Landau K. Optic nerve sheath meningiomas in patients with neurofibromatosis type 2. *Arch Ophthalmol*. 2006;124(3):379-385. doi:10.1001/archophth.124.3.379.
 26. Feucht M, Griffiths B, Niemuller I, et al. Neurofibromatosis 2 leads to higher incidence of strabismological and neuro-ophthalmological disorders. *Acta Ophthalmol*. Dec 2008;86(8):882-6. doi:10.1111/j.1600-0420.2007.01088.x
 27. Evans DG, Birch JM, Ramsden RT. Paediatric presentation of type 2 neurofibromatosis. *Arch Dis Child*. Dec 1999;81(6):496-9. doi:10.1136/adc.81.6.496
 28. Arden-Holmes S, Fisher G, North K. Neurofibromatosis Type 2: Presentation, Major Complications, and Management, With a Focus on the Pediatric Age Group. *Journal of Child Neurology*. 2017;32(1):9-22. doi:10.1177/0883073816666736

อาการแสดงจำเพาะทางตาที่นำไปสู่การวินิจฉัยโรคท้าวแสนปมชนิดที่สองชนิดเกิดเร็ว



Pittaya Phamonvaechavan, MD¹
พิทยา ภมรเวชวรรณ, พ.บ.¹



Subongkoch Subhadhirasakul MD¹
สุบงกช ศุภีรสกุล, พ.บ.¹



Rawi Jongpipatchai, MD¹
รวี จงพิพัฒน์ชัย, พ.บ.¹



Supathida Jiamsawad, MD¹
ศุภิตา เจียมสวัสดิ์, พ.บ.¹

บทคัดย่อ:

ภูมิหลัง: โรคท้าวแสนปมชนิดที่ 2 (Neurofibromatosis type 2 หรือ NF2) เป็นโรคทางพันธุกรรมที่พบน้อย ซึ่งมีลักษณะเด่นคือการเกิดเนื้องอกในระบบประสาทส่วนกลาง โดยเฉพาะเนื้องอกเส้นประสาท (Schwannoma) และเนื้องอกเยื่อหุ้มสมอง (Meningioma) การวินิจฉัยมักล่าช้าเนื่องจากอาการที่แสดงออกต่างกันไป ซึ่งอาการทางตาอาจเป็นอาการแสดงที่พบได้เร็วที่สุดในเด็ก

อาการและการดำเนินโรค: เด็กชายอายุ 4 ปี ถูกส่งตัวมาเพื่อตรวจตาเนื่องจากพบ café-au-lait macules หลายจุด ตรวจตาพบการมองเห็นลดลง ร่วมกับการ มี bilateral iris mammillation และ left retinal hamartoma ทำให้บ่งถึงโรค NF2 ผู้ป่วยได้รับแว่นตาเป็นการรักษาเบื้องต้น แต่ผู้ป่วยไม่ได้มาตรวจตามนัด เมื่อกลับมาตรวจซ้ำตอนอายุ 8 ปี พบว่าการมองเห็นในตาซ้ายมัวมากขึ้น ตรวจพบ flame-like epiretinal membrane (ERM) ในตาขวา และพบ combined hamartoma of the retina and retinal pigment epithelium (CHRRPE) ในตาซ้าย Magnetic Resonance Imaging (MRI) ยืนยัน Schwannoma หลายจุด และ optic nerve sheath meningioma (ONSM) ที่ตาซ้าย และได้รับการวินิจฉัยว่าเป็น NF2 เมื่ออายุ 10 ปี

การอภิปราย: ผู้ป่วย NF2 ในเด็กมักมีอาการแสดงทางตาเกิดขึ้นก่อนอาการทางระบบประสาท เช่น cortical cataract, ERM, CHRRPE และ ONSMs การรู้จักอาการแสดงทางตาเหล่านี้ มีความสำคัญในการวินิจฉัยและจัดการโรคอย่างทันท่วงที ซึ่งอาจช่วยลดอัตราการสูญเสียการมองเห็นได้

สรุป: ในผู้ป่วยรายนี้ ได้แสดงถึงความสำคัญของการตรวจตาอย่างละเอียดของผู้ป่วย NF2 ในเด็ก การวินิจฉัยได้ตั้งแต่อายุยังน้อย จะสามารถนำไปสู่การรักษาที่เหมาะสมได้ในหลายสาขาวิชา และเป็นการเพิ่มโอกาสการรักษาผู้ป่วย NF2 ในเด็ก

คำสำคัญ: ฮามาร์โตมาของจอตา, จักษุวิทยาเด็ก, เนื้องอกของเยื่อหุ้มเส้นประสาทตา, โรคท้าวแสนปม, โรคท้าวแสนปมชนิดที่สอง

Footnotes and Financial Disclosures

Originally receive: 15/8/2024

Final revision: 19/12/2025

Accepted: 19/12/2025

Corresponding author: Pittaya Phamonvaechavan, MD

Department of Ophthalmology, Faculty of Medicine Siriraj Hospital, Mahidol University, Bangkok 10700, Thailand

เรื่อง Choroidal Vasculature Index Changes after Treatment of Persistent Central Serous Chorioretinopathy with either Spironolactone or Half-Dose Photodynamic Therapy

หน้า 64

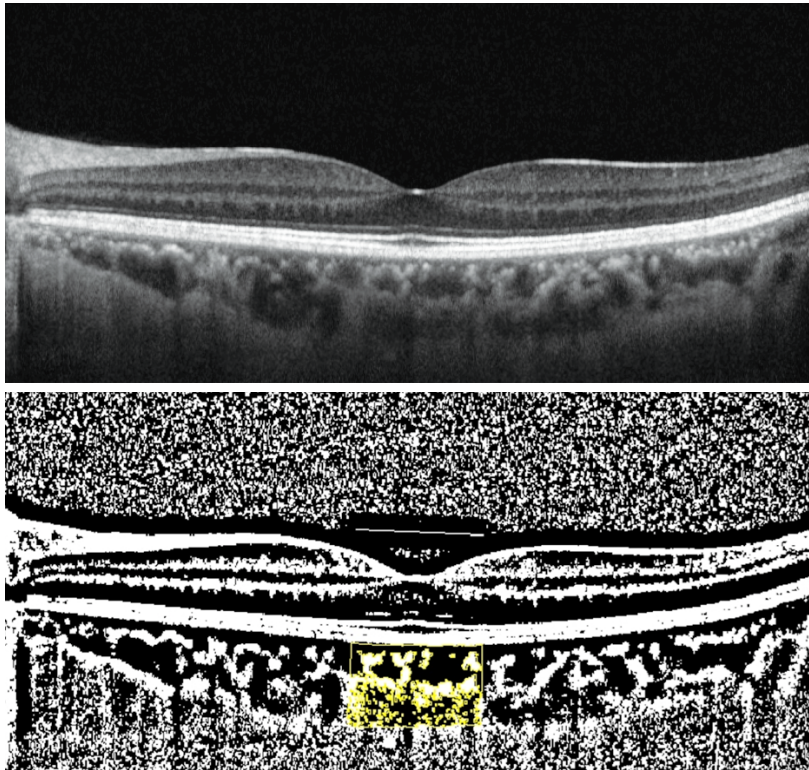
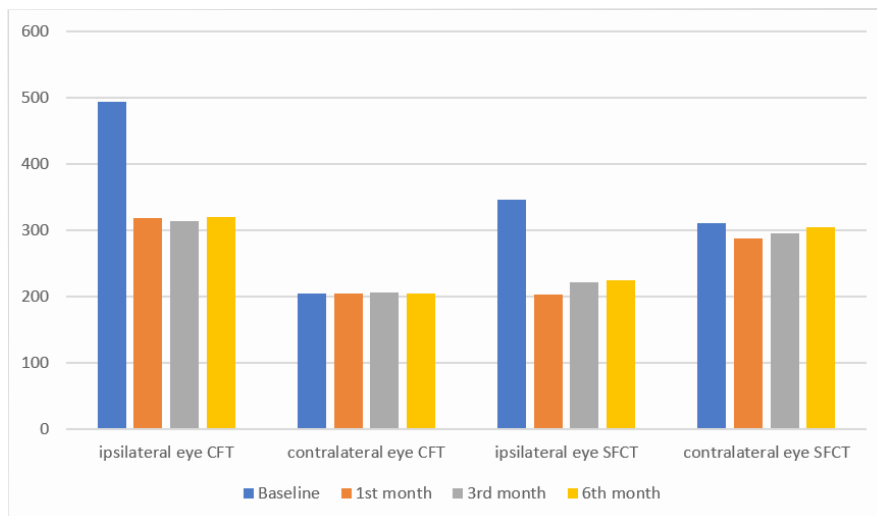


Figure 1 Enhanced-depth optical coherence tomography central B-scan of the left eye (left panel). Following binarization, the choroid was divided into dark (vascular lumen) and bright (stroma) pixels. A region of interest (highlighted in yellow) with a width of 1,500 μm centered on the foveal center was selected to compute the choroidal vascularity index (CVI). #Unpaired t-test for continuous data and Chi-square test for categorical data

เรื่อง Effects of Dexamethasone Implant on Contralateral Central Foveal and Subfoveal Choroidal Thickness in Unilateral Uveitic Macular Edema

หน้า 77



Graphic 1 Change of CFT and SFCT measurements of ipsilateral and contralateral eyes at baseline, 1st, 3rd and 6th month after intravitreal Ozurdex® implantation

เรื่อง Acute Unilateral Isolated Ptosis as a Complication of Frontal Sinusitis: A Case Report

หน้า 85



Figure 1 Photograph of the patient. The patient at initial presentation with left upper-eyelid ptosis.

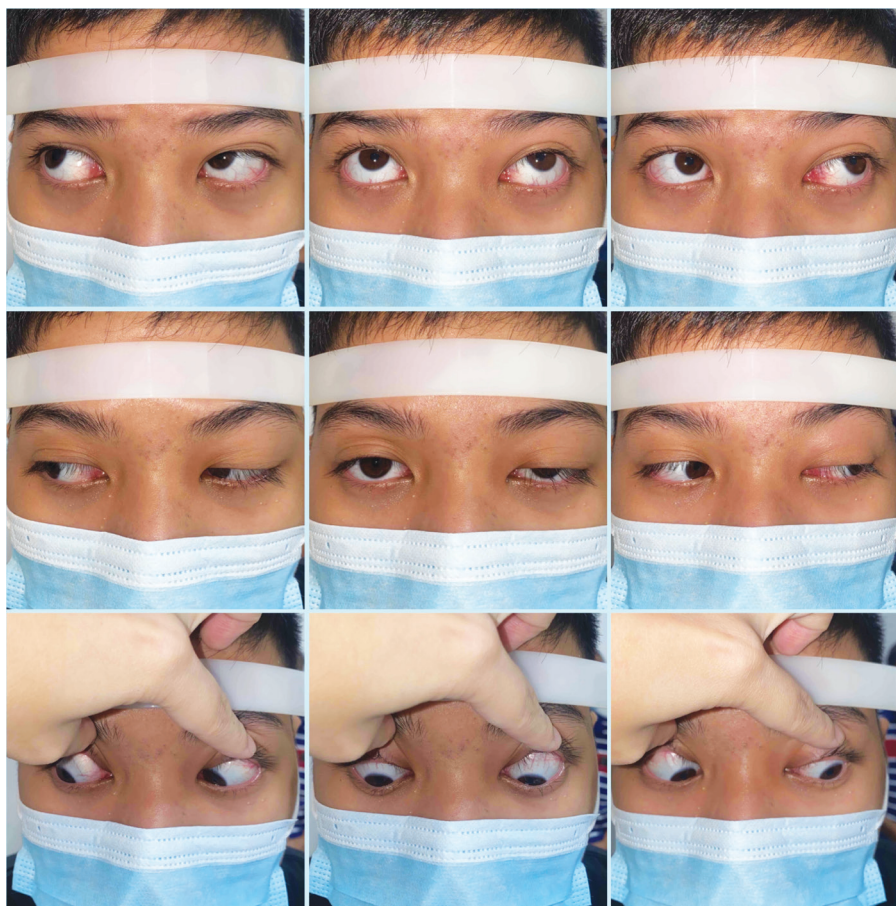


Figure 2 Photographs of the patient. The nine cardinal positions of gaze.

เรื่อง Adult Orbital Xanthogranuloma: A Case Report

หน้า 92

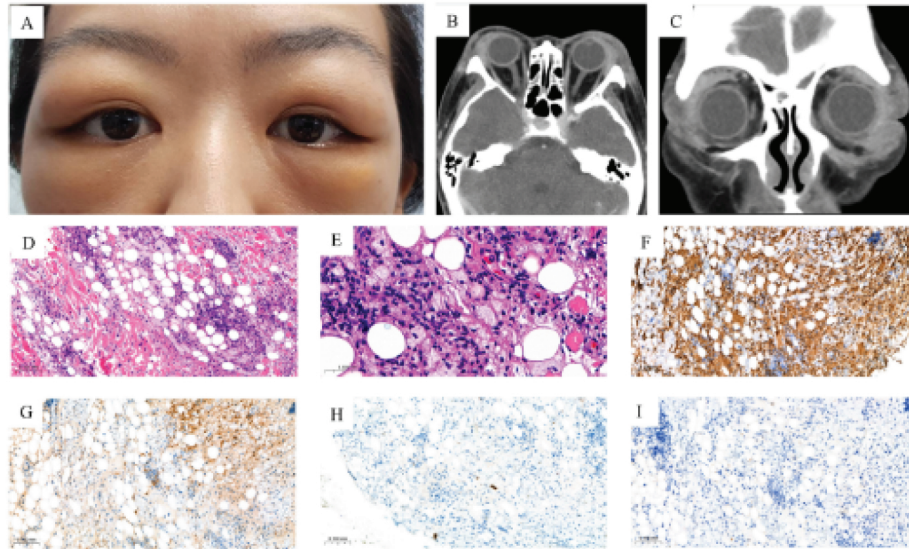


Figure 1 A 39-year-old Thai woman presented progressive painless bilateral upper and lower eyelids swelling for 5 years and yellow skin discoloration at left lower eyelid for 2 years. Bilateral lacrimal gland enlargements and proptosis of her right eye were detected. There were no other signs and symptoms of infection (A). CT scan of the orbit showed mild enhancing infiltrative soft tissue in both periorbital areas and lacrimal glands without bony destruction (B, C). An incisional biopsy was conducted at the area of yellow skin discoloration, which revealed the presence of foamy macrophages and small lymphoid cells in H & E (D, E), Positive for CD 68 (F), factor XIIIa (G) and negative for CD1a (H) and S100 (I). No systemic involvement has been detected in this patient. Based on her clinical and histopathological feature, a diagnosis of adult orbital xanthogranulomatous disease. adult xanthogranulomatous disease of the orbit (AOX) subtype was made. Oral prednisolone 1 mg/kg/day was prescribed. The patient responded well to it.

หน้า 93



Figure 2 The patient at the 3-month follow-up after oral prednisolone treatment.

เรื่อง Specific Ocular Findings Leading to the Diagnosis of Early-Onset Neurofibromatosis Type 2

หน้า 99

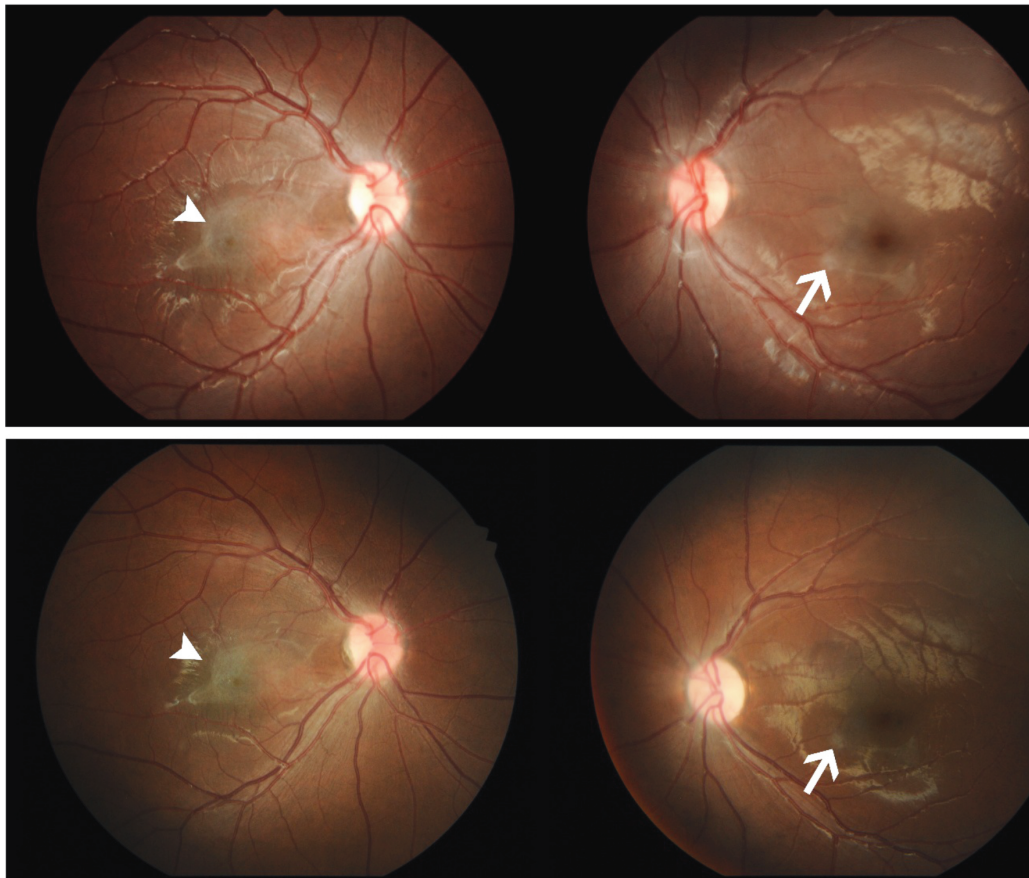


Figure 1 (A) Initial fundus photography of a 4-year-old boy showing an epiretinal membrane (arrowhead) in the right eye and a retinal hamartoma (arrow) in the left eye. (B) Fundus photography at age 10 years depicting an epiretinal membrane (arrowhead) in the right eye, along with a pale optic disc and a retinal hamartoma (arrow) in the left eye.

หน้า 100

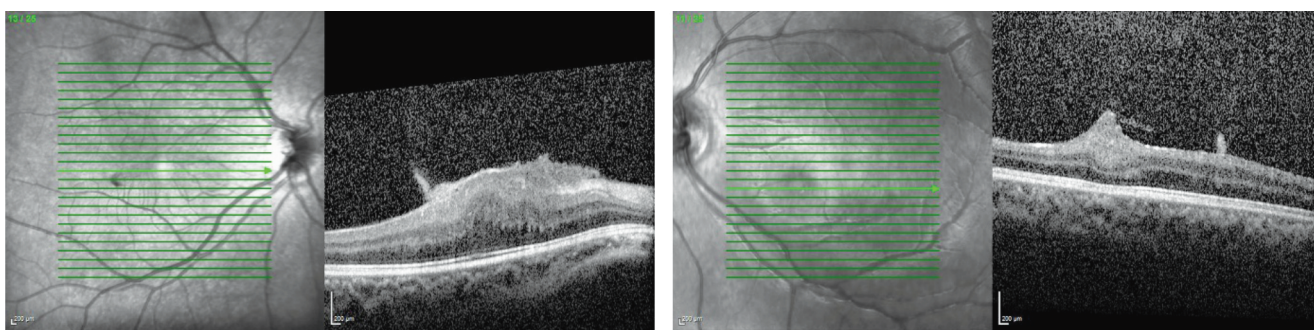


Figure 2 Spectral-domain optical coherence tomography illustrates the distinctive flame-like pattern of an epiretinal membrane extending into the vitreous in the right eye, and a combined hamartoma involving the retina and retinal pigment epithelium in the left eye.

หน้า 101

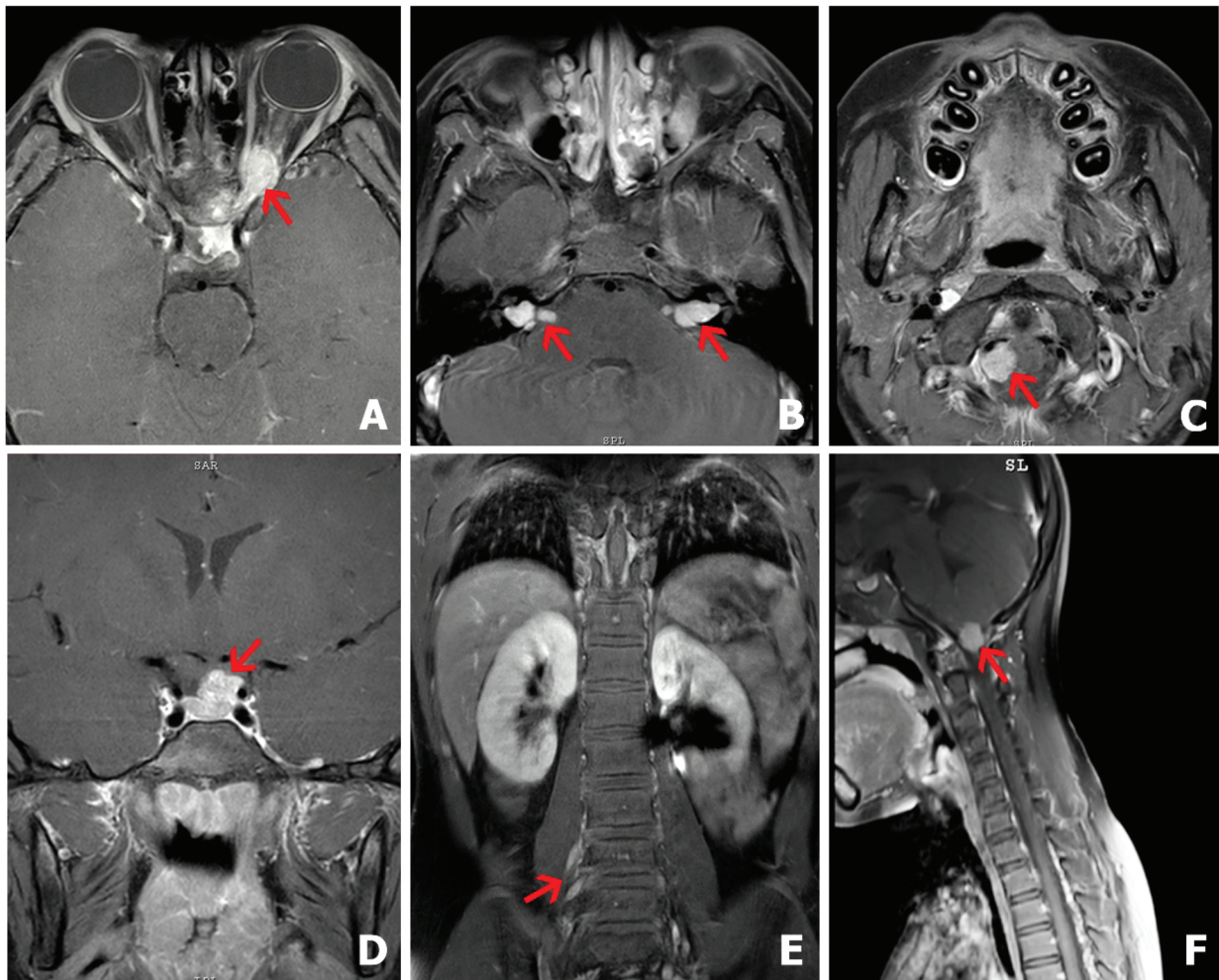


Figure 3 MRI T1-weighted images postgadolinium in axial and coronal planes demonstrate multiple tumors. (A) Left optic nerve sheath meningioma; (B) bilateral vestibular schwannomas (arrows); (C) right-sided meningioma at the cervicomedullary junction in axial and (F) sagittal views; (D) schwannoma on the left planum sphenoidale, partially extending to the pituitary fossa; and (E) meningiomas at the L4 and L5 nerve roots (arrows).

ดัชนีผู้เขียน

ชญาณี เพ็ญเพียร, 32 ชูพงศ์ อิศระณรงค์พันธ์, 1	ช	มงคล อูยประเสริฐกุล, 91	ม
ดวงใจ ดวงฤทธิ์, 32	ด	รวี จงพิพัฒน์ชัย, 21, 97	ร
ธนกฤต สรสิทธิ์, 32	ธ	วิราภา เสนารักษ์, 41	ว
นนทพันธ์ ณรงค์, 32	น	ศักดิ์ชัย วงศกิตติรักษ์, 32 ศุภธิดา เจียมสวัสดิ์, 21, 97	ศ
บุษยณัฐ พวงศรีเจริญ, 83	บ	สิริภา ทิพย์รัตน์, 49 สุนิสา สิ้นตุวงศ์, 91 สุธี อนันต์ประเสริฐ, 32 สุบงกช ศุภีรสกุล, 97	ส
ปพิชญา เต็มภัทราโชค, 91	ป		
พิทยา ภมรเวชวรรณ, 21, 97	พ	อรรถพล ยงวิกุล, 41	อ

Authors Index

	A		
Agrawal R, 61		Phamonvaechavan P, 21, 97	
Ananprasert S, 32		Piripyakootorn S, 61	
		Pooliam J, 61	
		Puangricharoeng B, 83	
	B		
Baris ME, 75			S
		Sadda SR, 61	
	C	Sensarak W, 41	
Chanwimol K, 61		Sintuwong S, 91	
		Sorasit T, 32	
	D	Subhadhirasakul S, 97	
Damla M, 75			T
Duangrithi D, 32		Taweebanjongsin W, 61	
	I	Temphattharachok P, 91	
Issaranarongpan C, 1		Tipparut S, 49	
	J		U
Jiamsawad S, 21, 97		Uiprasertkul M, 91	
Jongpipatchai R, 21, 97			V
	N	Vongkittirux S, 32	
Narong N, 32			Y
	P	Yonvikul A, 41	
Paul M, 10			
Penpian C, 32			